UNCLASSIFIED

SECURITY CLASSIFICATION OF THIS PAGE (When Data Entered)

(14) AFIT-CI-76-68

(6)

AD A027127

REPORT DOCUMENTATION PAGE

READ INSTRUCTIONS BEFORE COMPLETING FORM

1. REPORT NUMBER: CI-76-68
2. GOVT ACCESSION NO.
3. RECIPIENT'S CATALOG NUMBER
4. TITLE (and Subtitle): THE BASIC THEORY OF PHASED ARRAYS WITH A DISCUSSION OF THE BLIND ANGLE
5. TYPE OF REPORT & PERIOD COVERED: Master of Science Thesis
6. PERFORMING ORG. REPORT NUMBER
7. AUTHOR(s): (10) LAWRENCE DAVID BECKER, MAJOR, USAF — (9) Master's Thesis,
8. CONTRACT OR GRANT NUMBER(s): (1)
9. PERFORMING ORGANIZATION NAME AND ADDRESS: AFIT Student at the University of Illinois, Urbana, Illinois
10. PROGRAM ELEMENT, PROJECT, TASK AREA & WORK UNIT NUMBERS
11. CONTROLLING OFFICE NAME AND ADDRESS: AFIT/CI, Wright-Patterson AFB OH 45433
12. REPORT DATE: May 1976
13. NUMBER OF PAGES: 74 pages
14. MONITORING AGENCY NAME & ADDRESS (if different from Controlling Office): (12) 82p.
15. SECURITY CLASS. (of this report): Unclassified
15a. DECLASSIFICATION/DOWNGRADING SCHEDULE
16. DISTRIBUTION STATEMENT (of this Report): Approved for Public Release; Distribution Unlimited
17. DISTRIBUTION STATEMENT (of the abstract entered in Block 20, if different from Report)
18. SUPPLEMENTARY NOTES: JERRY C. HIX, Captain, USAF, Director of Information, AFIT — APPROVED FOR PUBLIC RELEASE AFR 190-17.
19. KEY WORDS (Continue on reverse side if necessary and identify by block number)
20. ABSTRACT (Continue on reverse side if necessary and identify by block number): Attached

(9)

DD FORM 1 JAN 73 1473 EDITION OF 1 NOV 65 IS OBSOLETE

UNCLASSIFIED 012 200 LB

SECURITY CLASSIFICATION OF THIS PAGE (When Data Entered)

INSTRUCTIONS FOR PREPARATION OF REPORT DOCUMENTATION PAGE

RESPONSIBILITY. The controlling DoD office will be responsible for completion of the Report Documentation Page, DD Form 1473, in all technical reports prepared by or for DoD organizations.

CLASSIFICATION. Since this Report Documentation Page, DD Form 1473, is used in preparing announcements, bibliographies, and data banks, it should be unclassified if possible. If a classification is required, identify the classified items on the page by the appropriate symbol.

COMPLETION GUIDE

General. Make Blocks 1, 4, 5, 6, 7, 11, 13, 15, and 16 agree with the corresponding information on the report cover. Leave Blocks 2 and 3 blank.

Block 1. Report Number. Enter the unique alphanumeric report number shown on the cover.

Block 2. Government Accession No. Leave Blank. This space is for use by the Defense Documentation Center.

Block 3. Recipient's Catalog Number. Leave blank. This space is for the use of the report recipient to assist in future retrieval of the document.

Block 4. Title and Subtitle. Enter the title in all capital letters exactly as it appears on the publication. Titles should be unclassified whenever possible. Write out the English equivalent for Greek letters and mathematical symbols in the title *(see "Abstracting Scientific and Technical Reports of Defense-sponsored RDT/E," AD-667 000)*. If the report has a subtitle, this subtitle should follow the main title, be separated by a comma or semicolon if appropriate, and be initially capitalized. If a publication has a title in a foreign language, translate the title into English and follow the English translation with the title in the original language. Make every effort to simplify the title before publication.

Block 5. Type of Report and Period Covered. Indicate here whether report is interim, final, etc., and, if applicable, inclusive dates of period covered, such as the life of a contract covered in a final contractor report.

Block 6. Performing Organization Report Number. Only numbers other than the official report number shown in Block 1, such as series numbers for in-house reports or a contractor/grantee number assigned by him, will be placed in this space. If no such numbers are used, leave this space blank.

Block 7. Author*(s)*. Include corresponding information from the report cover. Give the name*(s)* of the author*(s)* in conventional order *(for example, John R. Doe or, if author prefers, J. Robert Doe)*. In addition, list the affiliation of an author if it differs from that of the performing organization.

Block 8. Contract or Grant Number*(s)*. For a contractor or grantee report, enter the complete contract or grant number*(s)* under which the work reported was accomplished. Leave blank in in-house reports.

Block 9. Performing Organization Name and Address. For in-house reports enter the name and address, including office symbol, of the performing activity. For contractor or grantee reports enter the name and address of the contractor or grantee who prepared the report and identify the appropriate corporate division, school, laboratory, etc., of the author. List city, state, and ZIP Code.

Block 10. Program Element, Project, Task Area, and Work Unit Numbers. Enter here the number code from the applicable Department of Defense form, such as the DD Form 1498, "Research and Technology Work Unit Summary" or the DD Form 1634, "Research and Development Planning Summary," which identifies the program element, project, task area, and work unit or equivalent under which the work was authorized.

Block 11. Controlling Office Name and Address. Enter the full, official name and address, including office symbol, of the controlling office. *(Equates to funding/sponsoring agency. For definition see DoD Directive 5200.20, "Distribution Statements on Technical Documents.")*

Block 12. Report Date. Enter here the day, month, and year or month and year as shown on the cover.

Block 13. Number of Pages. Enter the total number of pages.

Block 14. Monitoring Agency Name and Address *(if different from Controlling Office)*. For use when the controlling or funding office does not directly administer a project, contract, or grant, but delegates the administrative responsibility to another organization.

Blocks 15 & 15a. Security Classification of the Report: Declassification/Downgrading Schedule of the Report. Enter in 15 the highest classification of the report. If appropriate, enter in 15a the declassification/downgrading schedule of the report, using the abbreviations for declassification/downgrading schedules listed in paragraph 4-207 of DoD 5200.1-R.

Block 16. Distribution Statement of the Report. Insert here the applicable distribution statement of the report from DoD Directive 5200.20, "Distribution Statements on Technical Documents."

Block 17. Distribution Statement *(of the abstract entered in Block 20, if different from the distribution statement of the report)*. Insert here the applicable distribution statement of the abstract from DoD Directive 5200.20, "Distribution Statements on Technical Documents."

Block 18. Supplementary Notes. Enter information not included elsewhere but useful, such as: Prepared in cooperation with . . . Translation of *(or by)* . . . Presented at conference of . . . To be published in . . .

Block 19. Key Words. Select terms or short phrases that identify the principal subjects covered in the report, and are sufficiently specific and precise to be used as index entries for cataloging, conforming to standard terminology. The DoD "Thesaurus of Engineering and Scientific Terms" *(TEST)*, AD-672 000, can be helpful.

Block 20. Abstract. The abstract should be a brief *(not to exceed 200 words)* factual summary of the most significant information contained in the report. If possible, the abstract of a classified report should be unclassified and the abstract to an unclassified report should consist of publicly- releasable information. If the report contains a significant bibliography or literature survey, mention it here. For information on preparing abstracts see "Abstracting Scientific and Technical Reports of Defense-Sponsored RDT&E," AD-667 000.

★ U.S. GOVERNMENT PRINTING OFFICE : 1973—729-091/1431 3-1

THE BASIC THEORY OF PHASED ARRAYS WITH A DISCUSSION OF THE BLIND ANGLE

BY

LAWRENCE DAVID BECKER

Abstract: This report reviews the underlying theory of the phased array and then examines one of its most limiting problems--the blind angle. The theory of the phased array is developed by studying a simple two element array and then progressing to multi-element arrays. Following this, the progressive phase shift is incorporated into the driving currents and its result examined.

The blind angle phenomenon is presented and then a physical reason for its occurrence is sought. The mutual coupling concept is demonstrated by examining mutual impedance as a function of spacing. Then the two predominate theories, surface wave and modal, offering a physical insight into the phenomenon are examined. Considerable attention is devoted to the "Ghost Mode Hypothesis" of Oliner, et al. and the work of Louis Stark.

UNIVERSITY OF ILLINOIS AT URBANA-CHAMPAIGN

THE GRADUATE COLLEGE

May, 1976

WE HEREBY RECOMMEND THAT THE THESIS BY

LAWRENCE DAVID BECKER

ENTITLED THE BASIC THEORY OF PHASED ARRAYS

WITH A DISCUSSION OF THE BLIND ANGLE

BE ACCEPTED IN PARTIAL FULFILLMENT OF THE REQUIREMENTS FOR

THE DEGREE OF MASTER OF SCIENCE

Paul W. Klock
Director of Thesis Research

Earl Jordan
Head of Department

Committee on Final Examination†

Chairman

† Required for doctor's degree but not for master's.

D517

B

THE BASIC THEORY OF PHASED ARRAYS WITH A DISCUSSION OF THE BLIND ANGLE

BY

LAWRENCE DAVID BECKER

B.S., University of Illinois, 1975

THESIS

Submitted in partial fulfillment of the requirements
for the degree of Master of Science in Electrical Engineering
in the Graduate College of the
University of Illinois at Urbana-Champaign, 1976

Urbana, Illinois

ACKNOWLEDGEMENT

Prior to actually starting this report, I must take time to publicly acknowledge and thank two people. The first, Dr. Paul Klock, my advisor, kept me going and provided direction when I reached a state of utter confusion. His ability to point out concepts without appearing to do so will long be appreciated. The second is Dr. Ed Mast, who worked so long and hard to help me understand much of what I had read. Both of these men contributed so freely of their time and energies that it is impossible to repay them. All I can do is say, "thank you."

TABLE OF CONTENTS

LIST OF ILLUSTRATIONS

LIST OF ILLUSTRATIONS (Cont.)

INTRODUCTION

The last quarter century has witnessed the introduction of many new devices in the electronics field. Few, however, match the potential of the antenna array systems for enhancing capability in the fields of radar and communications. The arrays, and specifically the phased arrays, provide a means for scanning large areas of space in extremely short periods of time. They allow beam shapes to be varied for different applications from the same system. By scanning electronically, they remove the problems associated with mechanical scanning, specifically the starting and stopping of directional antennas. The advantages to be gained by these applications are almost limitless. However, to make use of these systems requires a modicum of understanding of their operation. Unfortunately, most of the literature on this subject is written on such a plane that the undergraduate student never obtains a thorough understanding of the basic physics involved in the array theory. Therefore, the primary purpose of this paper is to present this basic theory in such a manner that an undergraduate student with little more than a basic electric fields course will be able to garner a physical realization of this theory. Additionally, I have attempted to explain on approximately this same level one of the more serious problems that affect the phased arrays--the blind angle.

THE PHASED ARRAY ANTENNA

Radiation Pattern from a Dipole

As all technical papers must start with certain assumptions, I will assume that the reader has studied electromagnetic radiation and has come in contact with a dipole antenna. For those wishing a thorough treatment of this subject, I suggest they consult a book such as Rao[1] or Hayt.[2] If we use a short dipole, assume a constant current along its length, and choose the coordinate system and orientation of Figure 1 the electric field pattern at a large distance from the antenna (radiation or far field pattern) can be described analytically as:

$$E = K \frac{\sin\theta}{r} \text{ Volts/meter} \qquad (1)$$

This field is sketched in Figure 2. You will note that the pattern has no ϕ dependence but radiates its distinctive $\sin\theta$ pattern everywhere in a circle around the dipole.

Suppose we wished to keep the $\sin\theta$ pattern but wanted to stop radiation at various values of ϕ- to approximate the pattern shown in Figure 3. It seems apparent that some means is necessary for cancelling the radiation at $\phi = 0^{\circ}$ and 180°. This could be accomplished by placing perfect electric conductors around the dipole at these angles. In fact, that particular process is the basis for the parabolic reflectors you see used on radar antennas. However, you will recall that electromagnetic fields

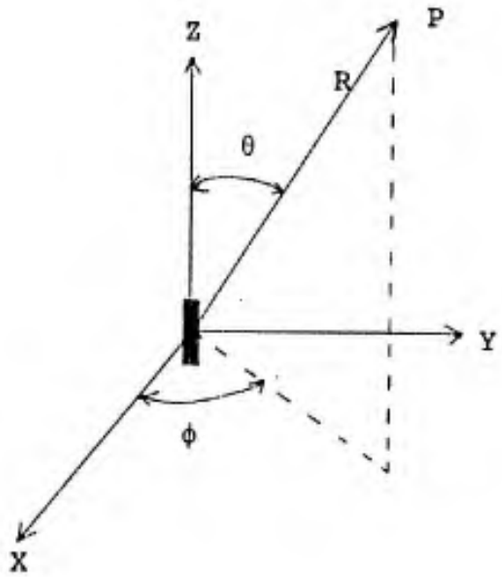

Fig. 1.--Coordinates and orientation

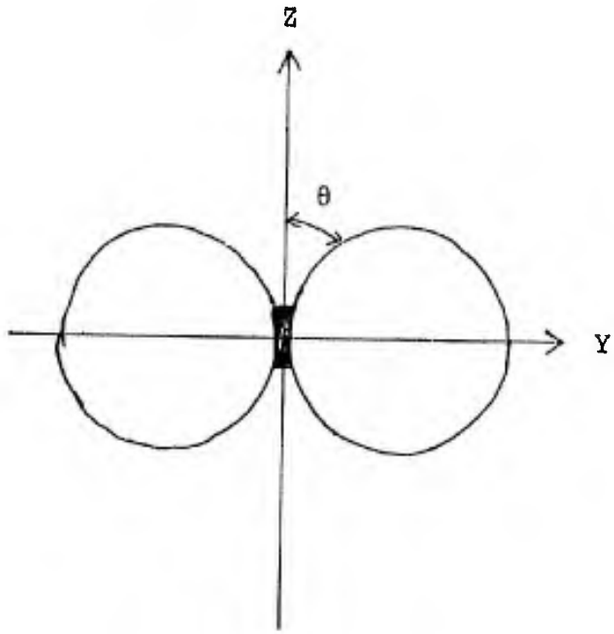

Fig. 2a.--|E| pattern as a function of θ

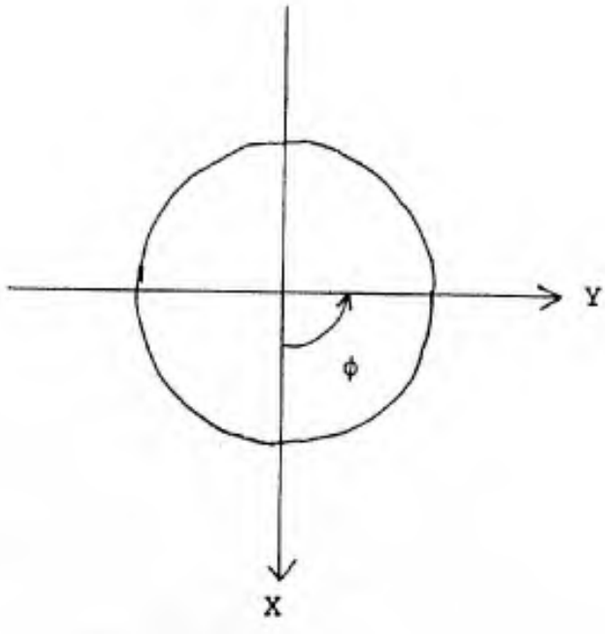

Fig. 2b.--|E| pattern as a function of ϕ

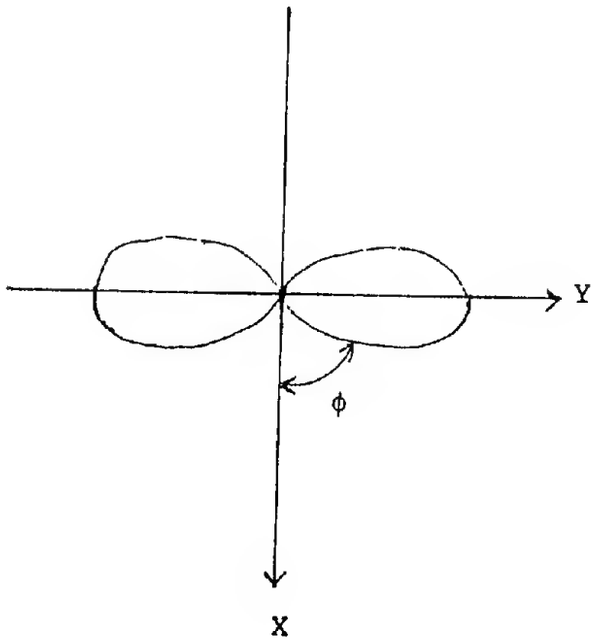

Fig. 3.--Desired pattern in XY plane

are linear and hence the theory of superposition can be applied. In this case, if we could add the negative of the dipole's radiated field to it at these chosen angles of ϕ, then we should be able to obtain the desired pattern.

Two Element Array

The problem with this plan is obtaining the negative of the dipole's pattern in only a few directions. To accomplish this it is necessary to recall that electromagnetic radiation travels at a finite velocity, and therefore, it takes time for radiation to move from the dipole to some exterior point. With this in mind, we examine the result of placing two identical short dipoles a small distance apart, for example, one half wavelength ($\lambda/2$). Next we will feed these dipoles from the same generator located equidistant from each of them so that the signal arrives at each antenna at the same time or, more simply, in phase. Also, we assume the generator produces a sinusoidal current of amplitude A and frequency ω_o.

Using Figure 4 as a reference, we pick an observation point A at some large distance from the two elements along the $\phi = 90^o$ line. You will note that at this point you are equidistant from both elements, so the radiated energy from each element reaches you at the same time. Hence, from superposition, the E field at the point is:

$$E_{TOTAL} = E_1 + E_2 \qquad (2)$$

Due to the way we chose to feed the elements

$$E_1 = E_2.$$

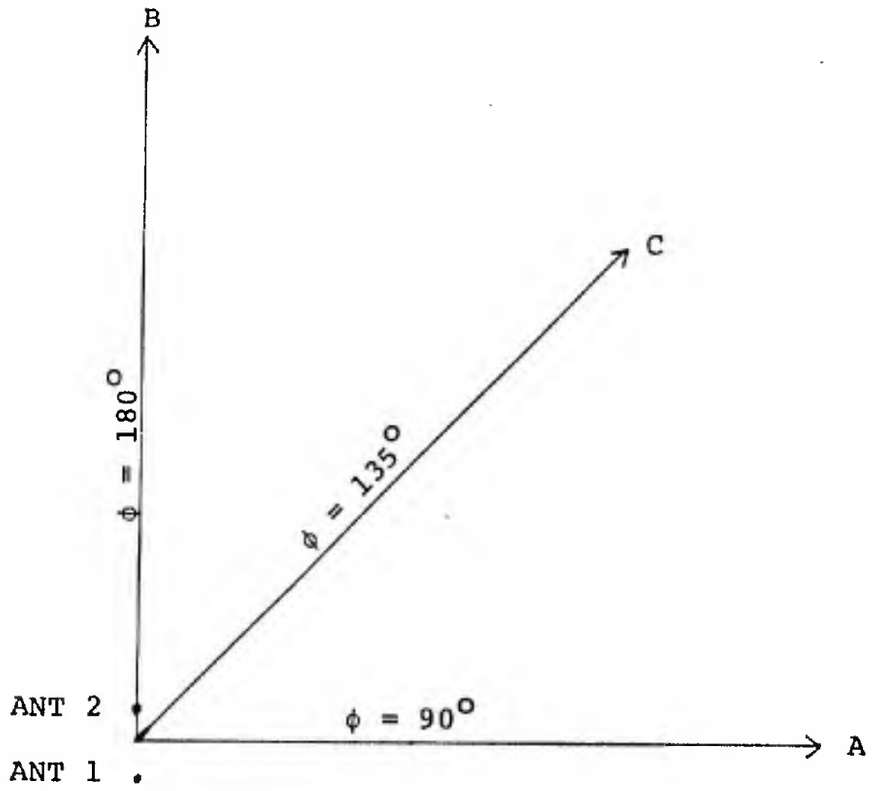

Fig. 4.--Observation points around a two element array

Therefore,

$$E_{TOTAL} = 2E_1.$$

Next, we choose an observation point B at the same distance but along the line $\phi = 180^{o}$. Continuing to feed the elements in phase we follow the radiated signal from element 1 (see Figure 4) as it moves toward our observation point. At time t_o, the signals at elements one and two are identical and we assume they are both at their maximum, A (see Figure 5a). As the wave, or signal, from element one starts toward the observation point, the field at element two continues to vary at the generator rate, Figure 5b. Assuming the medium between the elements is free space, then, at time t_2 (Figure 5c) when the radiated signal from element one has traveled the one half wavelength distance to element two, the current from the generator has moved through one half cycle and the signal at antenna 2 now has value -A. From this point on out to the observation point, the two signals travel together and again the total field is their sum. Hence, the field at any point outside the area between the elements and along the $\phi = 180^{o}$ line is:

$$E_{TOTAL} = E_1 + E_2,$$

$$= A + (-A),$$

$$= 0.$$

From symmetry the field along the $\phi = 270^{o}$ line is equal to the field along the $\phi = 90^{o}$ line; likewise, the $\phi = 0^{o}$ line equals the $\phi = 180^{o}$ line. We now have obtained the beginnings

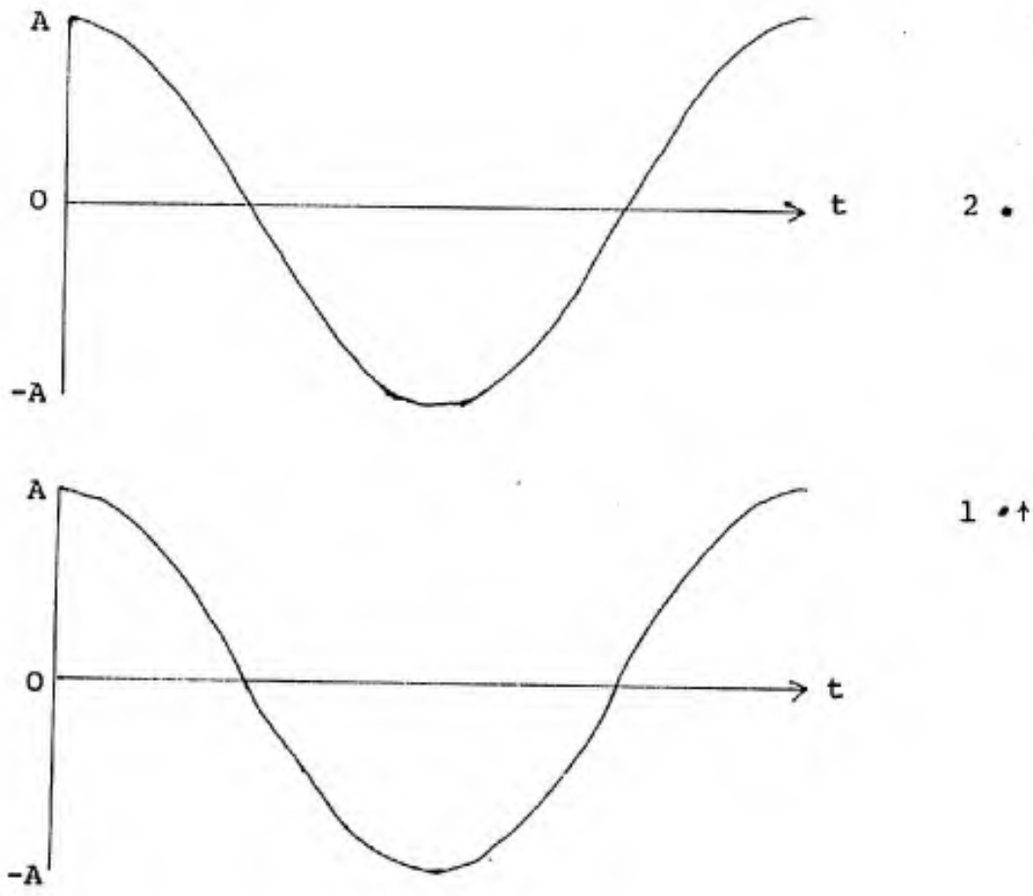

Fig. 5a.--Field amplitude at antennas 1 and 2 as a function of time.

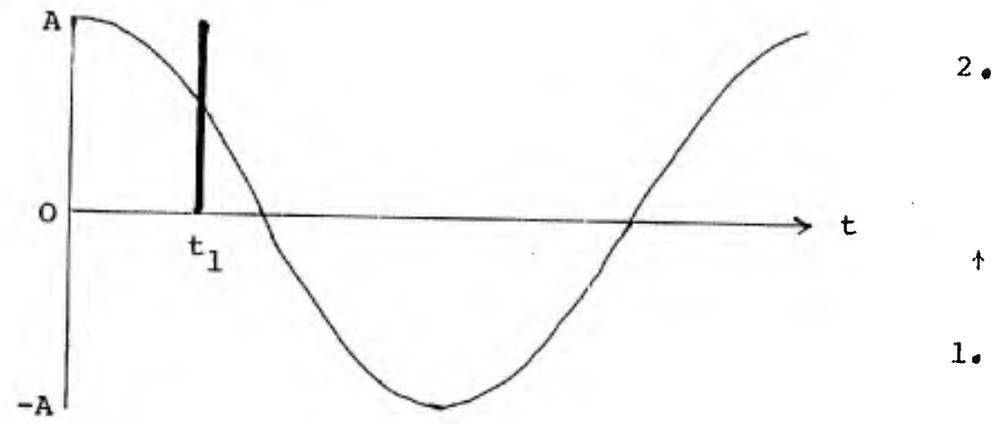

Fig. 5b.--Field amplitudes at t_1. Signal from antenna 1 has moved to position of arrow; antenna 2's field continues to change.

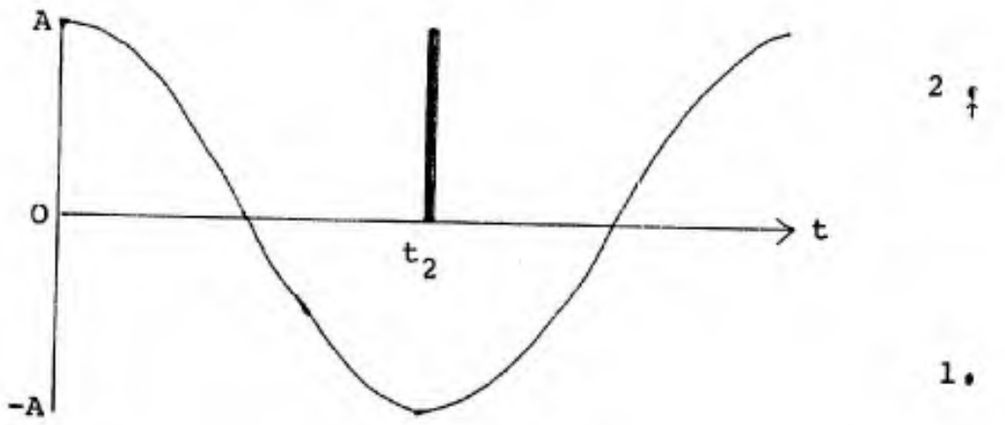

Fig. 5c.--Field amplitude at t_2. Signal from antenna 1 has reached antenna 2. Amplitudes are equal and opposite.

of the pattern we wanted, or at least we have a null at the $\phi = 0^{o}$ and 180^{o} points. To complete this analysis, we examine the field at some point C between $\phi = 90^{o}$ and 180^{o}, say 135^{o}. An examination of Figure 4 shows that the signals now won't actually travel the same distance as in the first case nor intercept the other radiating element as in the second case.

To analyze this situation, it is convenient to make the simplifying assumption that since the observation point is a large distance (in terms of wavelengths) from the center of the two elements, then the signals from the elements travel in essentially parallel paths to the observation point (much like light from a distant star to different points on the earth). See Appendix I for a discussion of the error involved in this assumption. Since the E fields add, what we need to find is the difference between the fields at the observation point. As was shown in the analysis of the $\phi = 180^{o}$ line, the difference between the fields is due only to the distance the signals must travel to reach the observation point. The parallel path assumption we made now enables this difference to be easily calculated using simple trigonometry.

In Figure 6 you see the paths the signals travel from each antenna. Since we assume that we are dealing with plane waves, we can draw a line perpendicular to the signal path of element 1. When this line, which represents a line of equal phase, reaches element two then the signals from that point on travel the same distance. Therefore, it is the distance signal one travels further than signal two which determines

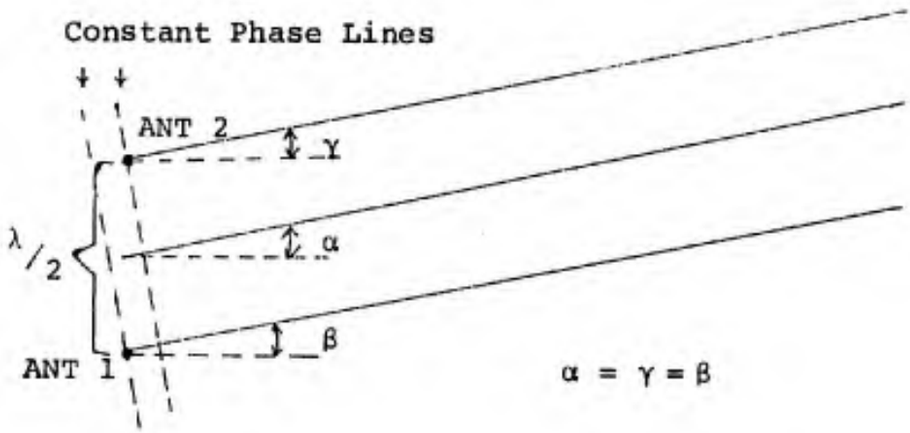

Fig. 6.--Additional distance antenna 1's signal travels

the total strength of the field at the observation point. We know the distance between elements one and two (½ wavelength); we also know the angle ϕ between the center of the array (the two elements) and the observation point. Due to the parallel lines this is the same angle for the radiated signals. Therefore, the distance differential (d) we seek is:

$$\begin{aligned} d &= \text{distance differential} \\ &= \text{distance between elements x } \cos(180-\phi), \\ &= -(\text{distance between elements x } \cos\phi). \end{aligned} \tag{3}$$

If we use the distance between elements in wavelengths, then we will obtain our distance differential in wavelengths.

From physics we know that one wavelength in space is the distance the wave travels in one complete time cycle of the generator. Therefore, if we know the distance in wavelengths, we can easily compute our position in the generator cycle and hence can know the amplitude of the current at that point. Then we know the amplitude of the field and can add the two together. At $\phi = 135^{\circ}$ the distance differential is:

$$\begin{aligned} d &= \lambda/2\ (-\cos 135), \\ d &= .35\lambda. \end{aligned}$$

So the distance through the cycle is .35 cycles.

We assumed the generator started on a maximum; so from Figure 7 the value of the amplitude is:

$$\begin{aligned} E_2 &= -.59A, \\ |E_{TOTAL}| &= A + (-.59A), \\ &= .41A. \end{aligned}$$

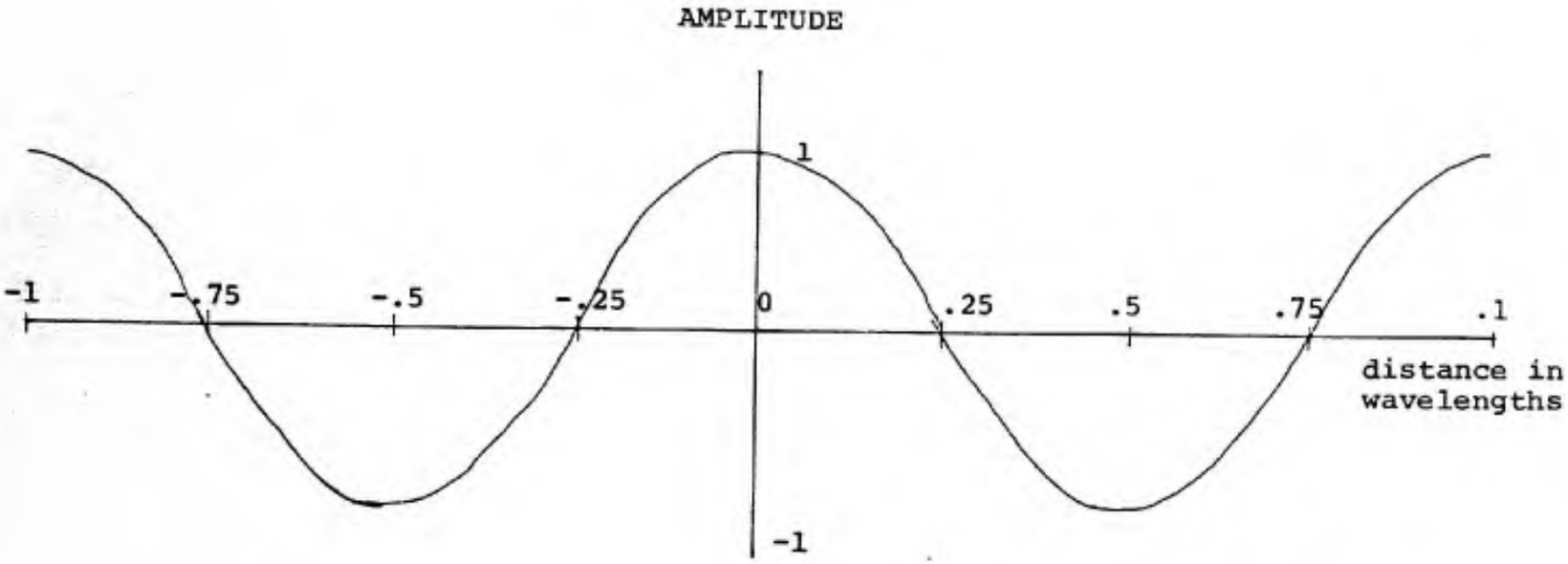

Fig. 7.--Amplitude of a wave as a function of distance along the wave

From the preceeding discussion, I think it is evident that the field will increase from 0 at $\phi = 0^{\circ}$ to a maximum of 2A at $\phi = 90^{\circ}$ and return to 0 at $\phi = 180^{\circ}$. The process will repeat for the range from $\phi = 180^{\circ}$ to $\phi = 360^{\circ}$. Thus by placing two dipoles one half wavelength apart and feeding them in phase we have obtained the pattern we wanted without adding any external modifications such as reflectors.

Let's stop for just a moment to consider what we have seen. By placing two antennas a ½ wavelength apart and feeding them in phase, we have caused a significant modification of the antenna pattern of the individual elements to occur. We saw that this modification occurred due to the addition of the radiated fields of the elements. We found that the difference in the field strength of each element was caused by the extra distance the wave had to travel to arrive at the same final position. Note also that the extra distance traveled is due to the location of one element relative to the other.

With this in mind, we examine the result of varying the spacing between the elements. We will change this distance by moving the elements along the $\phi = 0^{\circ}$ and 180° line. First, any movement of the elements along this line will not change the fact that a point on the $\phi = 90^{\circ}$ line from the center of the array is still equidistant from both antennas and hence, the fields there will always be in phase (arrive at same time) and yield twice the field of either element at that distance.

If we examine the field along the $\phi = 180^{\circ}$ line we will note an important result of varying the element spacing. At ½

wavelength the fields were 180° out of phase and cancelled, but at either smaller or larger spacing, the fields won't completely cancel and hence, we no longer have a null on this bearing. Figure 8 shows the total field at element 2 due to element 1 as a function of spacing. The first thing to notice from the figure is that the field is periodic of period one wavelength; also there is only one point within a one wavelength spacing where the fields go to zero. My choice of ½ wavelength spacing for the initial example should now be clear. Another result of using the $\lambda/2$ spacing is apparent if you examine equation (3) derived earlier; for convenience let:

s = distance between elements in wavelengths

then (2) $d = -(S \cos \phi)$ $\quad 0^\circ \leq \phi \leq 360^\circ$

Therefore with S = ½

ϕ	d
0	-½
90	0
180	½
270	0
360	-½

(5)

Using Figure 7 you will note that the amplitude of the field of one element at the other varies from:

d	amplitude
-½	-1
0	1
½	-1
0	1
-½	-1

Multiplying these values times E and adding them to the field of the other antenna yields the original pattern. Now if

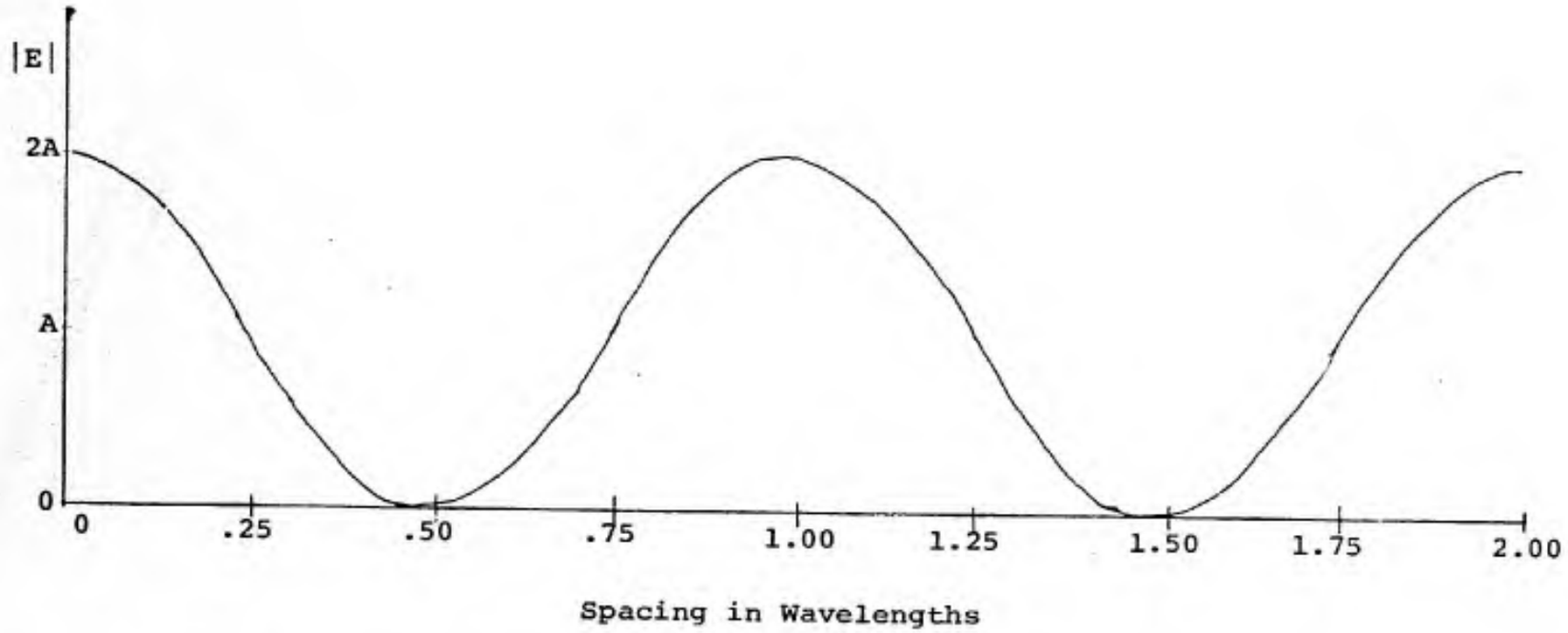

Fig. 8.--Total E field at antenna 2 due to separation from antenna 1

we make the spacing smaller, equation (2) shows that $|d|$ will stay less than $\lambda/2$. This will yield a pattern that has the same maximum at $\phi = 90^{o}$ and 270^{o} but never reaches a complete null at $\phi = 0^{o}$ and 180^{o} (Figure 9).

If we make the spacing greater than $\lambda/2$, equation (2) now shows that d will vary through a total distance greater than one wavelength. From Figure 7 you can see that the value of the field amplitude of the antenna at the observation point (relative to the amplitude of the field due to the other antenna) will vary from some number greater than -1 through -1 to 1 to -1 and on to the starting point and then back. To see this effect let's choose a separation of one wavelength. Using equation (3) and Figure 7 the following results are obtained:

ϕ	d	amplitude
0	-1	1
45	-.707	-.27
60	-.5	-1
90	0	1
120	.5	-1
135	.707	-.27
180	1	1
225	.707	-.27
240	.5	-1
270	0	1
300	-.5	-1
315	-.707	-.27
360	-1	1

Again assuming the field from one antenna is constant at 1 everywhere and adding the field obtained above, we obtain the pattern plotted in Figure 10. We still have the field maximums located at 90^{o} and 270^{o}, but we also have added maximums at 0^{o} and 180^{o}. The beams at 90^{o} and 270^{o} are called the main beam

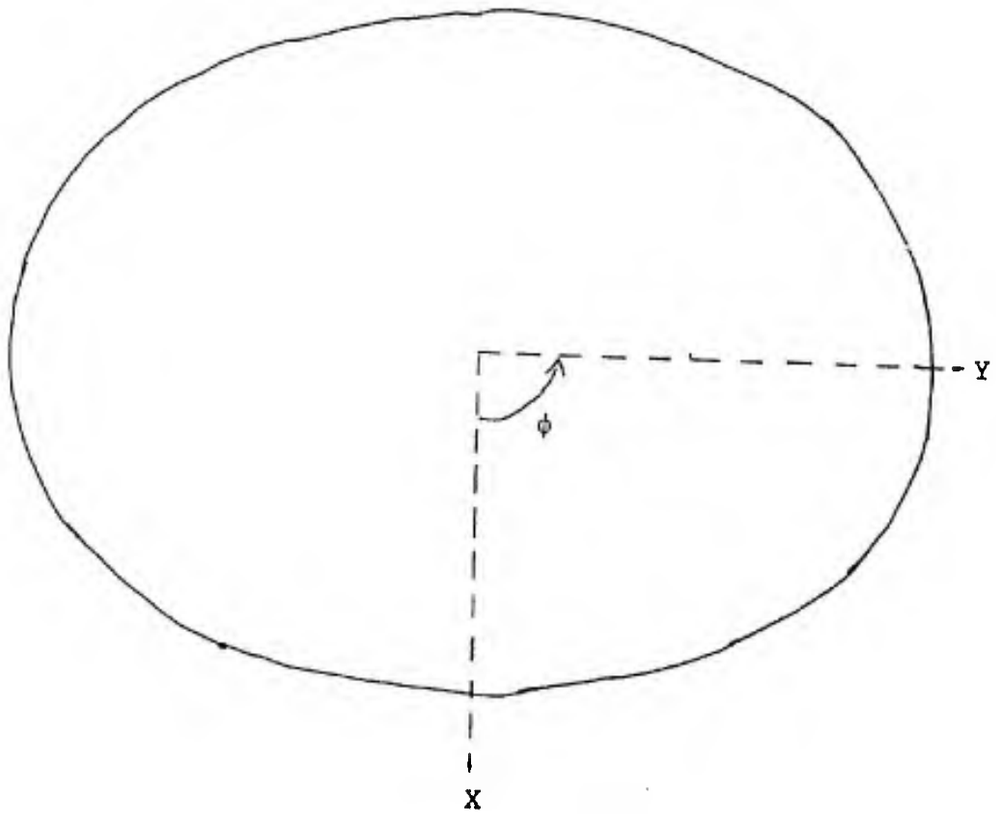

Fig. 9.--Pattern of a two element array with less than ½ wavelength separation.

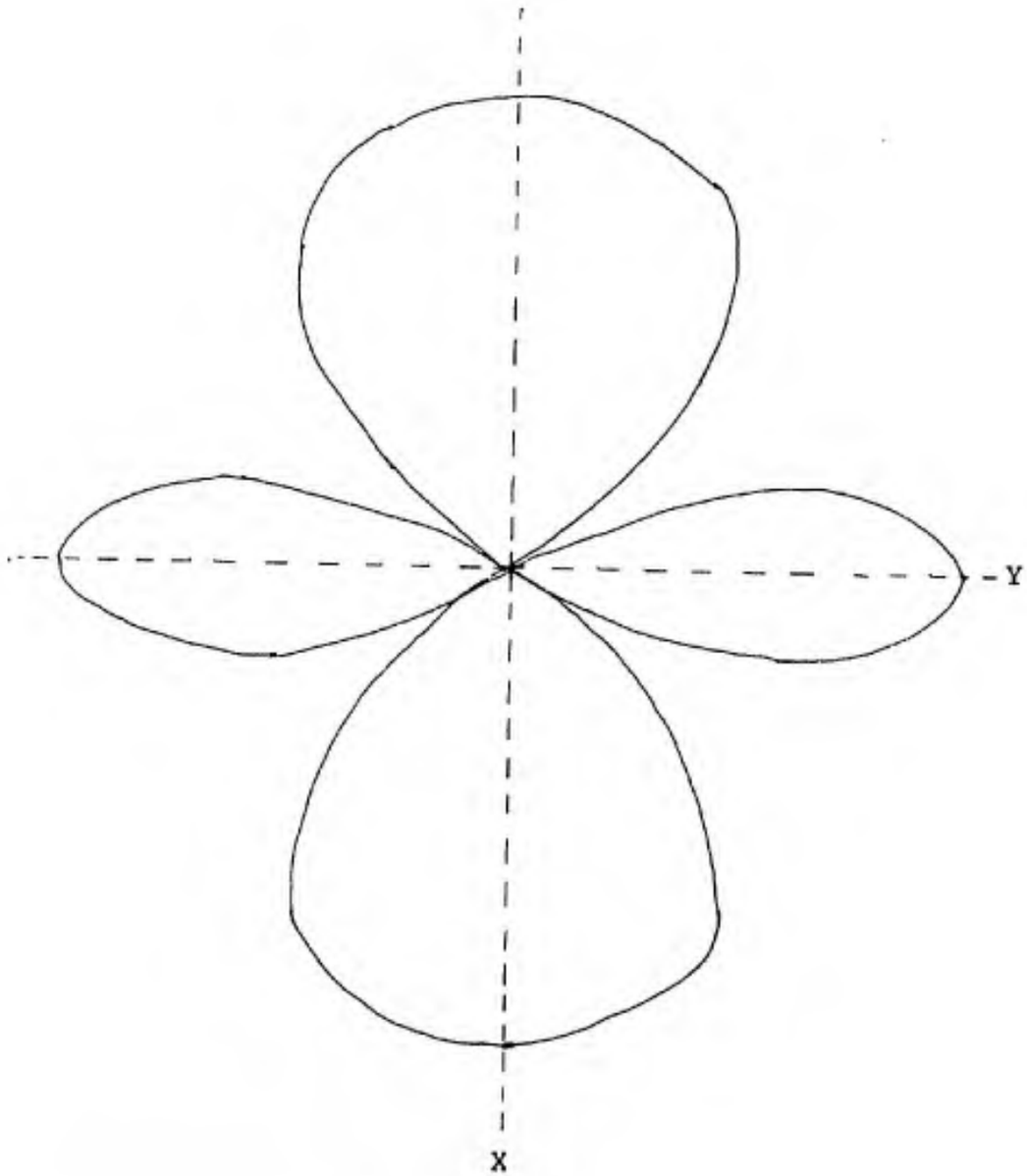

Fig. 10.--Radiation pattern of a two element array with one wavelength separation.

of the array because they are always there regardless of spacing, and the other beam is called a grating lobe. Normally the grating lobe is not desired since it reduces the radiated power in the direction of the main beam. If we continue to increase the interelement spacing, we will continue to add more grating lobes until, in the limit of infinite spacing, we obtain an infinite number of grating lobes--the original single element pattern.

Multi Element Array

When actual arrays are constructed they normally use many more than the two elements we have examined. However, the principles we have developed are still applicable; they are just applied to more elements. For illustration, let's examine a colinear four element array. To remain consistent, I will restrict the current to each element to be in phase and set the interelement spacing to be .75 wavelengths (see Figure 11). I have already demonstrated that the far field pattern is nothing more than the summation of the individual element patterns at any given point. Therefore, to find the pattern of this array we need do nothing more than determine a way of adding all the element patterns. Looking along the $\phi = 90^{o}$ line we see that as before the patterns all add in phase, giving us a maximum E field strength of 4 times the strength of one antenna. Along the $\phi = 180^{o}$ line let's examine the total field at antenna 4 to find the field radiated from the array. Let the field due to antenna four be a maximum of amplitude A. The field due to antenna 3 has traveled .75 λ; so, from Figure 7 it has amplitude 0. Likewise,

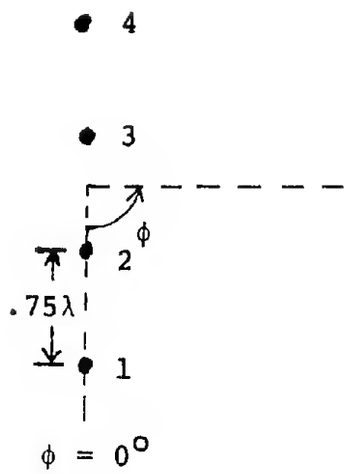

Fig. 11.--Arrangement of a four element array

antenna 2's signal travels 1.5 λ for an amplitude of -A and antenna 1's signal goes 2.25 λ for an amplitude of 0. This yields a total radiated strength of:

$$E_T = E_1 + E_2 + E_3 + E_4 = A\,[1 + 0 - 1 + 0],$$

$$E_T = 0,$$

which indicates a total null at this point. Examine now the $\phi = 120^{\circ}$ direction. Assuming again that the amplitude from antenna 4 is at a maximum of A then antenna 3's signal travels -d cos ϕ wavelength further, antenna 2's -2d cos ϕ, antenna 1's -3d cos ϕ. Using Figure 7 this yields a total field of:

$$E_T = A[-.7 + 0 + .7 + 1]$$

$$E_T = A.$$

Repeating this same process for a number of angles of ϕ, I obtained the values listed below; their plot is found in Figure 12.

ϕ	E_1/A	E_2/A	E_3/A	E_4/A	$\lvert E_T/A \rvert$
0	0	-1	0	1	0
10	.21	-.99	-.07	1	.15
20	.75	-.84	-.28	1	.63
30	.95	-.30	-.59	1	1.06
40	-.17	.59	-.89	1	.53
50	-.94	.97	-.99	1	.04
60	.71	0	-.71	1	1
70	.12	-1	-.04	1	.08
80	-.77	.07	.68	1	.98
90	1	1	1	1	4
100	-.77	.07	.68	1	.98
110	.12	-1.0	-.04	1	.08
120	.71	0	-.71	1	1
130	-.94	.97	-.99	1	.04
140	-.17	.59	-.89	1	.53
150	.95	-.30	-.59	1	1.06
160	.75	-.84	-.28	1	.63
170	.21	-.99	-.07	1	.15
180	0	-1	0	1	0

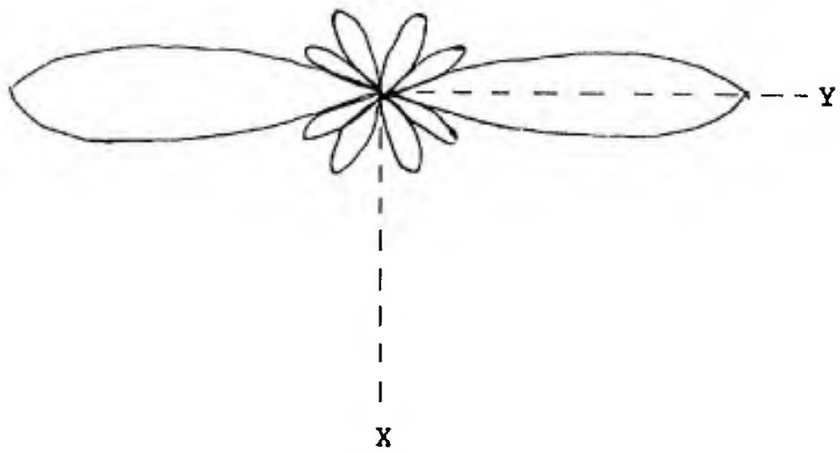

Fig. 12.--Radiation pattern of a four element array with 3/4 wavelength spacing.

The first thing that is apparent from Figure 12 is the symmetry. If we examine the range of ϕ from 0^{o} to 180^{o}, it is identical to the 180^{o}-360^{o} range. Therefore, let's examine the 0^{o}-180^{o} range. You will note that the largest or main lobe appears at the $\phi = 90^{o}$ position as it has done in both previous examples. This main beam is always broadside to the array and hence, this array is known as a broadside array. In addition to the main beam there are now smaller beams. These are known as the side-lobes and appear as local maximums between the nulls. In the case of the 4 element array both side lobes are the same magnitude. With larger arrays this is not generally the case. Unlike the example with one wavelength spacing this array produced no grating lobe. However, if we increased the interelement spacing sufficiently, in this case to one wavelength, then instead of the pattern in Figure 12, the side lobes would be closer together and a grating lobe would appear at $\phi = 0^{o}$ and 180^{o}. The pattern realized with this one wavelength spacing is shown in Figure 13. It was obtained as in the other examples, and the interested reader is urged to apply these methods to produce it.

As a result of the preceeding discussion, I believe we are now in a position to make a few general statements regarding antenna arrays. First, regardless of the number of antennas involved, the far field pattern is nothing more than a summation of the fields of the individual elements. Second, by feeding all the elements with in phase current the main beam always forms broadside to the array. The fact that the element currents are uniform in amplitude and differ at most by a phase constant has

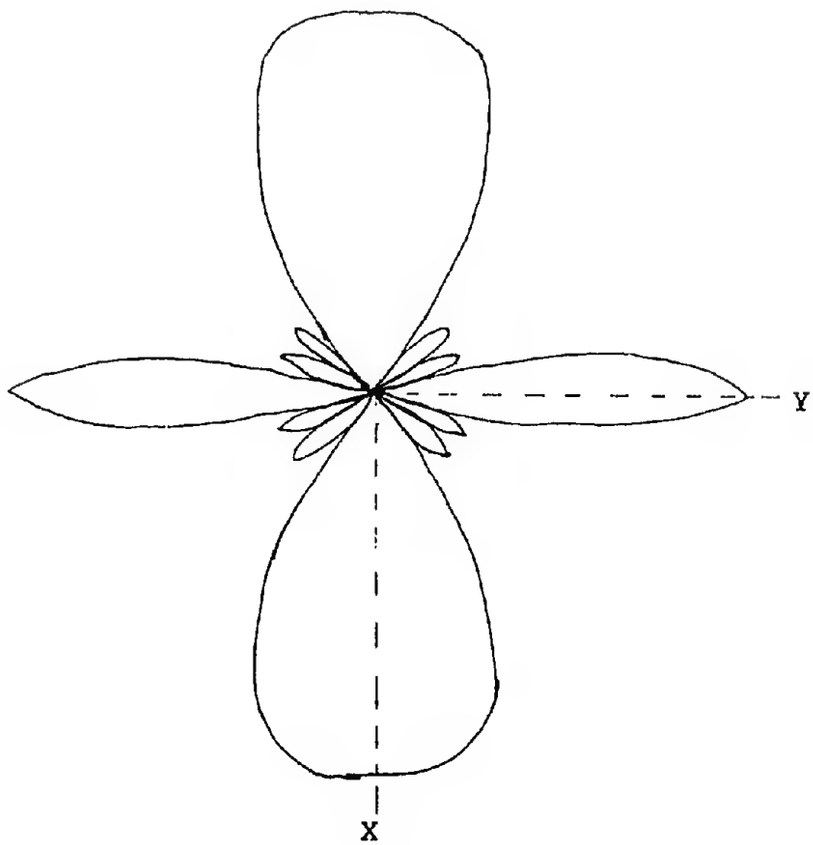

Fig. 13.--Radiation pattern of a four element array with one wavelength separation.

resulted in this type of array being called a uniform array.[3] Third, the addition of more elements spaced equidistant results in not only a narrower main lobe but the appearance of side lobes. Finally, varying the interelement spacing results in the changing of the side lobe position, of the beamwidth of the main beam, and, if the spacing is large enough, in the appearance of grating lobes.

Array Mathematics

It should be obvious by now that the method we have chosen for determining the far field pattern of our arrays is extremely cumbersome. Therefore, let us see if we can deduce a mathematical expression that will provide the desired information. We know that the E field in the far zone of a short dipole antenna oriented along the Z axis is given by:

$$E_\theta = \frac{jk\eta}{4\pi R} e^{-jkR} \sin\theta \int_V J \cdot dv \qquad (4)$$

If we assume a small antenna of length H with a uniform current distribution then:

$$\int_V J \cdot dv = \int_{-H/2}^{H/2} I \cdot dl = IH,$$

and

$$E_\theta = \frac{jk\eta IH}{4\pi R} e^{-jkR} \sin\theta \qquad (5)$$

where: $k = \frac{2\pi}{\lambda}$

η = intrinsic impedance of the medium

R = distance from element.

This, then, is the field from each of our array elements. However, you will recall that the variation in the pattern was

due to the different distance each ray had to travel to arrive at the same point. We already determined the difference between each element as d cos ϕ. Therefore, if we are computing the distance R from an element, we can represent it as:

$$R = r - d \cos \phi \tag{6}$$

where r = distance to point from reference

d = total spacing between reference and the element which we are concerned with

This then allows us to write the field for an array element as:

$$E = jk\eta IH \sin\theta \frac{e^{-jk[r-d\cos\phi]}}{4\pi R}$$

$$= jk\eta IH \sin\theta \, e^{-jkr} \frac{e^{jk\, d\cos\phi}}{4\pi R} \tag{7}$$

The R in the denominator is an attenuation factor rather than a phase factor as was R in the numerator. As a result the difference in distance for attenuation is negligible and so we make the approximation:

$$R = r,$$

which allows the field to be represented by:

$$E = jk\eta IH \sin\theta \frac{e^{+jk\, d\cos\phi}}{4\pi r} e^{-jkr} \tag{8}$$

From our example with 4 antennas all spaced the same distance apart we wrote the expression for the difference in distance traveled as -1d cos ϕ for the second antenna, -2d cos ϕ for the third, and -3d cos ϕ for the fourth. This process would continue indefinitely leading to the general conclusion that each field referenced to the first antenna could be shown to travel

$-(n-1)d \cos \phi$. In an n element array, therefore, we could write an expression for the total radiated field taking the first antenna for a reference with d = 0 as:

$$E_{TOTAL} = \frac{jk\eta IH}{4\pi r} e^{-jkr} \sin\theta \left[1 + e^{+jkd \cos \phi} + e^{+j2kd \cos \phi} + \ldots + e^{+j(n-1)kd \cos \phi}\right] \quad (9)$$

For ease of explanation let me make the following substitutions:

$$E_o = \frac{jk\eta IHe^{-jkr}}{4\pi r} \quad (10)$$

$$\psi = kd \cos \phi \quad (11)$$

Then we can rewrite the expression as:

$$E_{TOTAL} = E_o \sin\theta \left[1 + e^{+j\psi} + e^{+j2\psi} + \ldots + e^{+j(n-1)\psi}\right] \quad (12)$$

To avoid having to deal with negative fields we can use the relation:

$$\text{Power} = \frac{|E|^2}{\text{Resistance}} \quad (13)$$

$$\sqrt{P} = \frac{|E|}{\sqrt{\text{Resistance}}} \quad (14)$$

and deal only with the magnitude of the total E field. Therefore,

$$E_{TOTAL} = E_o \sin\theta \left|1 + e^{+j\psi} + e^{+j2\psi} + \ldots + e^{+j(n-1)\psi}\right| \quad (15)$$

The discerning reader will immediately recognize this as a geometric series. For those not so fortunate, this type of series is discussed in most advanced calculus books.[4] The end result is that this series can be written as:

$$E_{TOTAL} = E_o \sin\theta \left| \frac{1 - e^{+jn\psi}}{1 - e^{+j\psi}} \right| \tag{16}$$

and with a little manipulation (see Appendix II) this yields:

$$E_{TOTAL} = E_o \sin\theta \left| \frac{\sin \frac{n\psi}{2}}{\sin \frac{\psi}{2}} \right| \tag{17}$$

Examining this expression shows that we have the original field or pattern of a single element, $E_o \sin\theta$, multiplied by a factor $\left| \frac{\sin \frac{n\psi}{2}}{\sin \frac{\psi}{2}} \right|$ which came about solely as a result of the spacing between the elements or, more simply, the geometry of the array. The first term is known as the element pattern and the second as the array factor.

The development of this array factor makes it much simpler to compute the radiation pattern of the array than did our original approach. Whenever the denominator goes to zero, i.e., $\psi = 0, 2\pi, 4\pi \cdots$, the numerator will also be zero leading to a value of n. This corresponds to the main beam and grating lobes of the array. In between these points the numerator can reach zero while the denominator has some value, leading to a value zero for the field which is equivalent to a null. For example if $n = 4$ and $\psi = \pi/2$ then the numerator equals zero and the denominator is $\sin \pi/4$.

All that remains now to solve for the angles of ϕ that yield the maximum and the nulls is to determine the particular value of ψ that is required, and then solve for ϕ. As an example, let's look at our four element array with interelement spacing of $3\lambda/4$.

$$E_{TOTAL} \propto \left|\frac{\sin \frac{4\psi}{2}}{\sin \frac{\psi}{2}}\right| = \left|\frac{\sin 2\psi}{\sin \frac{\psi}{2}}\right| \tag{18}$$

1) The maximum occurs at $\psi = 0, \pm 2\pi, \pm 4\pi \cdots$

2) Nulls occur at $\sin 2\psi = 0$

$$2\psi = n\pi \quad n = \pm 1, \pm 2, \pm 3, \cdots$$

$$\psi = \frac{n\pi}{2}$$

3) Solve for ϕ.

$$\psi = kd \cos \phi$$

$$= \frac{2\pi}{\lambda} \cdot \frac{3\lambda}{4} \cos \phi$$

$$= \frac{3}{2} \pi \cos \phi$$

$$\phi = \cos^{-1} \frac{2\psi}{3\pi}$$

In 1 and 2 it is apparent that an infinite number of maximums and nulls occur. However, since ϕ can only range from 0^o to 360^o this places a bound on the number of maximums and nulls in this range. In fact, the arrays are symmetrical about the $\phi = 0^o$, 180^o plane so all that is necessary is to compute ϕ within this 180^o range.

4) Locate main beam: $\psi = 0$

$$\phi = \cos^{-1} \frac{2 \cdot 0}{3\pi}$$

$$\phi = 90^o$$

Look for grating lobes: $\psi = \pm 2\pi, \pm 4\pi, \cdots$

$$\phi = \cos^{-1} \pm \frac{2 \cdot 2\pi}{3\pi}$$

$$\phi = \cos^{-1} \pm \frac{4}{3}$$

No real angle ϕ can have a cosine greater than 1, therefore, there are no grating lobes.

5) Locate nulls: $\psi = \pm \pi/2, \pm \pi, \pm \frac{3\pi}{2}, \cdots\cdots$

$$\phi_1 = \cos^{-1} \frac{2 \cdot \pi/2}{3\pi}$$

$$\phi_1 = 70.5^{\circ}$$

$$\phi_2 = \cos^{-1} \frac{2 \cdot \pi}{3\pi}$$

$$\phi_2 = 48.2^{\circ}$$

$$\phi_3 = \cos^{-1} \frac{2 \cdot \frac{3\pi}{2}}{3\pi}$$

$$\phi_3 = 0$$

$$\phi_4 = \cos^{-1} \frac{2 \cdot 2\pi}{3\pi}$$

$$\phi_4 = \text{not defined}$$

Using negative n yields $\psi = -\pi/2, -\pi, -\frac{3\pi}{2}, \cdots$ resulting in:

$$\phi_{-1} = 109.5^{\circ}$$

$$\phi_{-2} = 131.8^{\circ}$$

$$\phi_{-3} = 180^{\circ}$$

Returning to our previous calculation for this array you will note that the results agree and the method is much simpler.

Another advantage in using this form is the rapidity with which you can determine the existence of a grating lobe. To accomplish this merely substitute the interelement spacing you wish to use and compute ψ for the complete range of ϕ. If ψ never reaches 2π, then no complete grating lobe exists. In the lexicon of the array people, the range of ψ that exists when ϕ is rotated through 360° is called the visible range of the array.[5]

We have now done a reasonably good job of emulating a reflector type antenna except for its ability to turn the reflector and move its beam. Obviously, it is impractical to move our array in order to move the beam. Therefore, let's examine the means of obtaining the pattern to see if some practical means of moving the beam can be found.

The Phased Array

In the broadside array developed earlier, we found that the main beam formed when the fields of all the antennas added in phase. At all other points this addition continued to take place but the fields were no longer in phase; consequently the total pattern strength declined. It seems reasonable then to conclude that we must find a means of obtaining this in phase addition at some point other than $\phi = 90^{\circ}$.

The reason we had this in phase addition was due to the signals leaving the antennas in phase and traveling the same distance to the observation point. If we move the observation point in the ϕ direction we change the distance that the individual signals must travel. For our argument, however, let's assume that we have our familiar two element array with ½ wavelength spacing, that we are at an observation point on the $\phi = 30^{\circ}$ line, and that the signals have arrived in phase. Next, let's return along the paths the signals traveled and determine what they must have looked like when they left the antenna.

The first signal, we will assume, traveled an integral number of wavelengths and we will use it for a reference. The second signal is in phase with the first, but it traveled an integral number of wavelengths plus d cos ϕ further. From our assumed array geometry this means the second signal traveled

$$d \cos \phi = \lambda/2 \cos 30^{\circ} = .43\lambda$$

further than the reference. To arrive in phase with the first it must have reached its maximum .43λ ahead of the reference.

Therefore, its current generator must be ahead of the reference generator by .43λ which translates to a phase lead of 154.8°. Consequently, if we run the generator of the second antenna 154.8° ahead of the reference antenna then the radiated fields will add in phase at $\phi = 30°$.

Changes in the beam direction, therefore, are accomplished by merely varying the relative phasing of the feed currents between elements. For illustrative purposes let's return to the four element array with .75 wavelength spacing. Initially we said the only difference between the individual radiated signals was the added distance they traveled. Now we must also take into account the phase difference. As I have just shown this phase difference translates to a spacing along a signal path so it has the same dimension as the kd cos ϕ and hence, can be added directly to it. Therefore, we can represent the difference in signals by:

$$kd \cos \phi + \alpha \tag{19}$$

where α is the phase difference. The current in any antenna relative to the adjacent antennas can be represented by:

$$I = A\, e^{j\alpha} \tag{20}$$

where: A = The magnitude of the feed current

α = Progressive phase change between elements

The radiated field of each element is then

$$E = \frac{jk\eta IHe^{-jkR}}{4\pi R} \sin \theta = \frac{jk\eta AHe^{-jkR}e^{j\alpha}}{4\pi R} \sin \theta \tag{21}$$

The total radiated field of all elements is:

$$E_{TOTAL} = \frac{jk\eta AHe^{-jkr}}{4\pi r} \sin\theta \left| 1 + e^{+jkd\cos\phi} e^{j\alpha} + e^{+j2kd\cos\phi} e^{j2\alpha} + e^{+j3kd\cos\phi} e^{j3\alpha} \right| \quad (22)$$

We have α, 2α, and 3α because α represents the phase shift between each element and is therefore $n\alpha$ away from the reference. Making the same type of substitution we did earlier we can represent the total field by:

$$\left|E_{TOTAL}\right| = \left| E_o \sin\theta \left[1 + e^{+j\psi} + e^{+j2\psi} + e^{+j3\psi}\right] \right| \quad (23)$$

$$E_o = \frac{jk\eta AHe^{-jkr}}{4\pi r}$$

$$\psi = kd\cos\phi + \alpha$$

or

$$\left|E_{TOTAL}\right| = \left|E_o \sin\theta\right| \left|\frac{\sin\frac{n\psi}{2}}{\sin\frac{\psi}{2}}\right| \quad (24)$$

Using a progressive phase shift α of -60^o yields

$$\psi = \frac{2\pi}{\lambda} \cdot \frac{3\lambda}{4} \cos\phi - 60^o$$

$$\phi = \cos^{-1}\frac{2(\psi+60^o)}{3\pi} = \cos^{-1}\left(\frac{\psi+60^o}{270^o}\right)$$

From the equation for E_{TOTAL} we see that the value of ψ for nulls, main beams, and grating lobes is still the same. Solving for ϕ yields:

Main beam: $\psi = 0$

$$\phi = \cos^{-1}\frac{60^o}{270^o}$$

$$\phi = 77.2^o$$

Grating Lobes: $\psi = \pm 2\pi, \pm 4\pi, \cdots$

$$\phi = \cos^{-1} \frac{360^\circ + 60^\circ}{270^\circ}$$

$\phi = \cos^{-1} 1.56 \rightarrow$ no grating lobe for $+ 2\pi$

$$\phi = \cos^{-1} \frac{-360^\circ + 60^\circ}{270^\circ}$$

$\phi = \cos^{-1} -1.1 \rightarrow$ no grating lobe for $- 2\pi$

Nulls: $\psi = \pm \pi/2, \pm \pi, \pm \frac{3\pi}{2} \pm 2\pi, \cdots$

$$\phi = \cos^{-1} \frac{\pm 90^\circ + 60^\circ}{270^\circ}$$

$\phi = 56^\circ, 96^\circ$

$$\phi = \cos^{-1} \frac{\pm 180^\circ + 60^\circ}{270^\circ}$$

$\phi = 27^\circ, 116^\circ$

$$\phi = \cos^{-1} \frac{\pm 270^\circ + 60^\circ}{270^\circ}$$

$\phi = 141^\circ$ for $\psi = -\frac{3\pi}{2}$, no real angle for $\psi = \frac{3\pi}{2}$

$\psi = \pm 2\pi$ does not yield a real angle

The main beam is now located at $\pm 77^\circ$, with nulls at $\pm 27^\circ$, $\pm 56^\circ$, $\pm 96^\circ$, $\pm 116^\circ$, $\pm 141^\circ$ and as before no grating lobe. This pattern is plotted in Figure 14. The values of the side lobes for this plot were estimated by picking the value of ϕ halfway between two adjacent nulls. This is not totally accurate but yields a close approximation. Comparing Figure 14 with Figure 12 you will see that the main lobe has shifted about 13° and the beginning of a grating lobe is apparent at 180°.

Since the symmetry is about the $\phi = 0^\circ$, 180° plane (due to the cos ϕ dependence in ψ) both the main beam and the back lobe are approaching each other. You may question what will

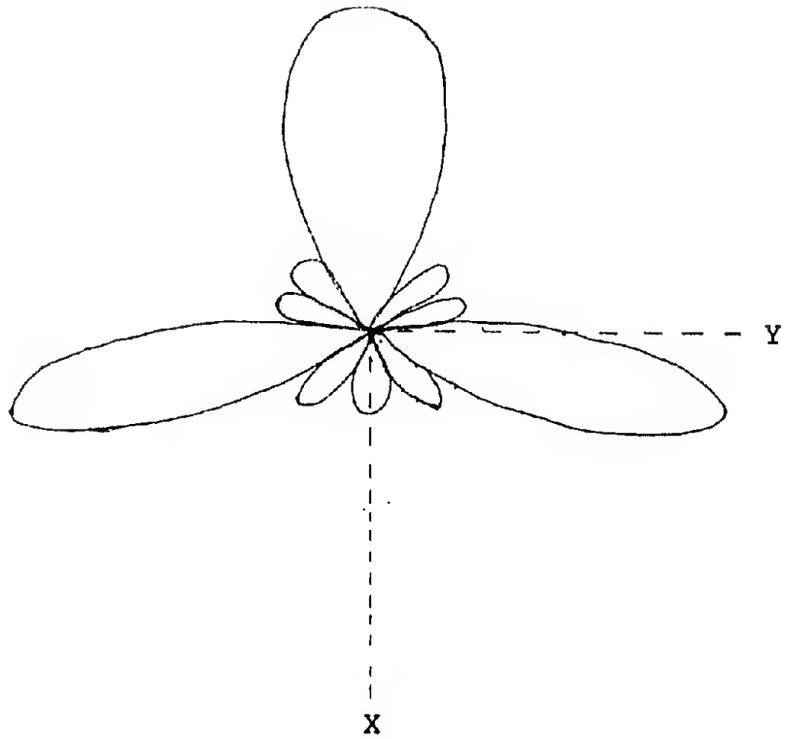

Fig. 14.--Radiation pattern of a four element array with 3/4 wavelength separation and a progressive phase shift α of -60^{o}.

occur when they overlap. As is apparent, this will occur when the main beam is pointing off the end of the array along the $\phi = 0^{o}$ direction. To obtain this we require ψ to be zero when $\phi = 0^{o}$. Putting these values into the 4 element array and solving for α yields:

$$\psi = kd \cos \phi + \alpha$$

$$\alpha = \psi - kd \cos \phi$$

$$\alpha = 0 - kd \cos (0)$$

$$\alpha = -kd$$

If $\alpha = +kd$ then the main beam forms along the $\phi = 180^{o}$ line. Figure 15 shows the pattern of the array with $\alpha = -270^{o}$. As predicted the main beam now appears along the line of the array or off the end. This firing off the end has led to the name of "End-Fire" for this configuration. You will note now the presence of grating lobes at $\pm 109^{o}$. Comparing Figure 15 with Figure 14 you will see that the total grating lobe has appeared without any change in the element spacing. Suppose we wished to suppress the grating lobes while still maintaining the end fire array. Examination of ψ showed that the end fire case required the phasing angle to equal ($\pm$ kd). Some minor manipulation yields:

$$\psi = kd \ (\cos \phi - 1) \qquad (25)$$

The grating lobe occurs when the denominator of the array factor equals zero.

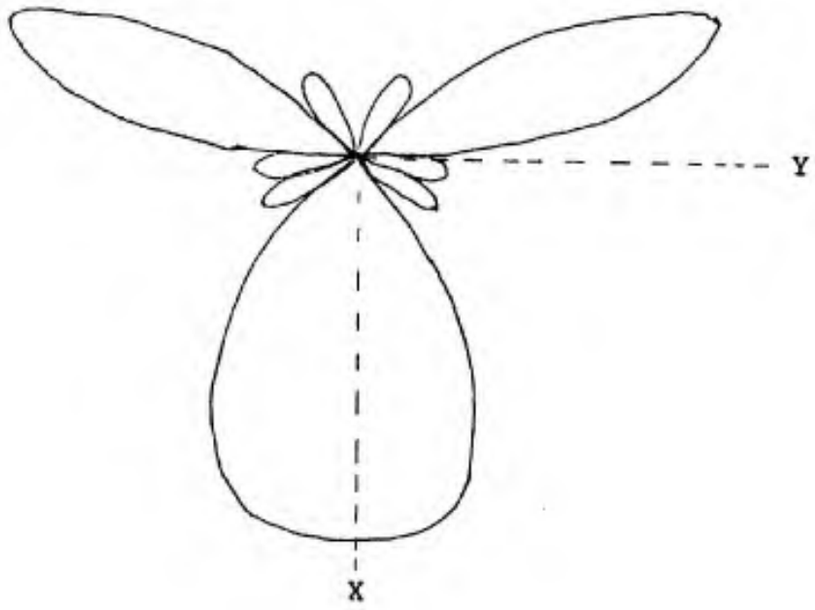

Fig. 15.--Radiation pattern of a four element array with 3/4 wavelength separation and a progressive phase shift of -270°.

$$\sin \frac{\psi}{2} = 0 \Rightarrow \psi = 0,\ n2\pi$$

$$kd\ (\cos \phi - 1) = n2\pi \quad \text{(1st grating lobe } n = 1\text{)}$$

$$kd = \frac{2\pi}{\cos \phi - 1}$$

$$d = \frac{\lambda}{\cos \phi - 1}$$

If we do not want a grating lobe then set $\phi = 180^{\circ}$ and solve for d.

$$|d| < \frac{\lambda}{2}$$

Using the same procedure on the broadside array yields a maximum spacing without a grating lobe of:

$$|d| < 1\lambda$$

What is immediately obvious is that the maximum spacing required for a no grating lobe condition is less for the end fire than the broadside case. As long as we are dealing with fixed beam arrays this really presents no problem since we would attempt to build it as close to broadside as possible. However, as you have probably deduced, what we have actually developed is a basis for sweeping the beam. If we could devise a way for varying the phase of the driving currents, then we could move the beam to any point we so desired. The excursion of our beam would then be the important point in determining the interelement spacing. A discussion of the means of changing the phase and hence, the beam location is beyond the scope of this paper. The process, though, is not a limiting factor and can be accomplished by simply using a series of delay lines between the generator and each element. This would not provide a continuously variable

beam but would allow a discrete set of beam locations. Nevertheless, we have succeeded in synthesizing the rotating radar reflector antenna by an array of stationary antennas.

Let's pause here for a moment and consider what we have developed. From the preceeding discussion you should now have a rather thorough understanding of the physics of phased array radars. You have seen the development of the interaction of the radiated fields that is the direct causal factor in the beam formation. You have seen the development of the underlying theory that allows the beam to be electronically scanned to any direction off the array. You have seen the effect on the array of adding elements and varying the element spacing. You have learned the meaning of side lobe, visible region, broadside and endfire array. What you have not, however, been exposed to is a much larger body of information. When arrays are considered, seldom will you find yourself dealing with only one dimension. We have not considered beam broadening as the array is scanned. You must also learn the process of pattern multiplication, a useful tool for designing arrays. We have only examined a colinear array of short dipoles while the real world concerns itself with arrays of slots, horns, spirals and every imaginable type of antenna arranged in an almost infinite number of geometries. My purpose, however, is not to scare you away from the subject but hopefully to whet your appetite so that you will pursue these challenging areas. I believe that if you understand the basics I presented, you can attack these other areas with the

confidence that comes from knowing that all they represent are applications of this basic theory.

You are probably now asking, "Why, if these phased arrays are so great, do I continue to see rotatable fixed beam antennas?" Unfortunately, as you have probably guessed, the simple explanations that I have provided are pure theory and have not addressed the practical problems that do exist. Although the problems that do exist are basically the same ones that apply to any antenna, there is one that merits special attention because it is found only in arrays.

THE BLIND ANGLE

When an array beam is swept across the entire array, i.e., from $\phi = 0^{o}$ to 180^{o}, we find that as the beam approaches certain angles, called blind angles, it goes through sharp reductions in radiated power. After the particular angle is passed the beam just as suddenly re-appears or regains its expected level.

In order to explain this phenomenon we must develop a reason for its occurrence and then examine it. I believe that the explanations can be reduced to two very general ones:

a) the power is being stored and not radiated

b) the power is being reflected and not radiated

In case (a) if the power is being stored then we must invent an infinite means of storage. This arises from the fact that in none of the literature I have examined has a case of a beam forming after a finite period of time been found or even proposed. Therefore, if the power is being stored, the storage medium must have an infinite capacity. While I have found nothing to disprove this idea I don't believe it offers any real understanding of the problem. Consequently, let us look at case b.

This reason is attractive because it permits a very wide latitude in our explanations. It requires only that some means of producing a mismatch between the feed and the antenna or

between the antenna and the surrounding medium be developed. From the theory we developed earlier a means of developing this mismatch is not available. Once we leave this theoretical realm and examine the real array we find a non-predicted development. Let's take an infinite array and terminate each element in a matched load so that no reflections can occur. Then connect a generator across the center element in place of the load and measure the radiation pattern. From our earlier theory we would expect to find the pattern to be identical with the pattern of the single element; in the case of a short dipole, a $\sin\theta$ variation with ϕ symmetry. However, actual measured results show that this is not the case.[6,7] What is obtained is a pattern with definite variations of the field in the ϕ plane (Figure 16). The only modification that we have made to the element is to include it in proximity to other elements. By terminating these other elements in matched loads we expect no reflections to occur. Thus, how do we explain this obvious interaction? A term in common usage to explain this is "mutual coupling."

Mutual Coupling

This concept shouldn't be new to you. When you were studying circuits you encountered a coupling concept in treating inductors. There was no physical connection between two coils but they did display a definite effect from each other. When we consider coupling between antenna elements we may or may not be discussing the same exact phenomena, but we do find a definite interaction between two physically unconnected elements. Carter[8] in 1932

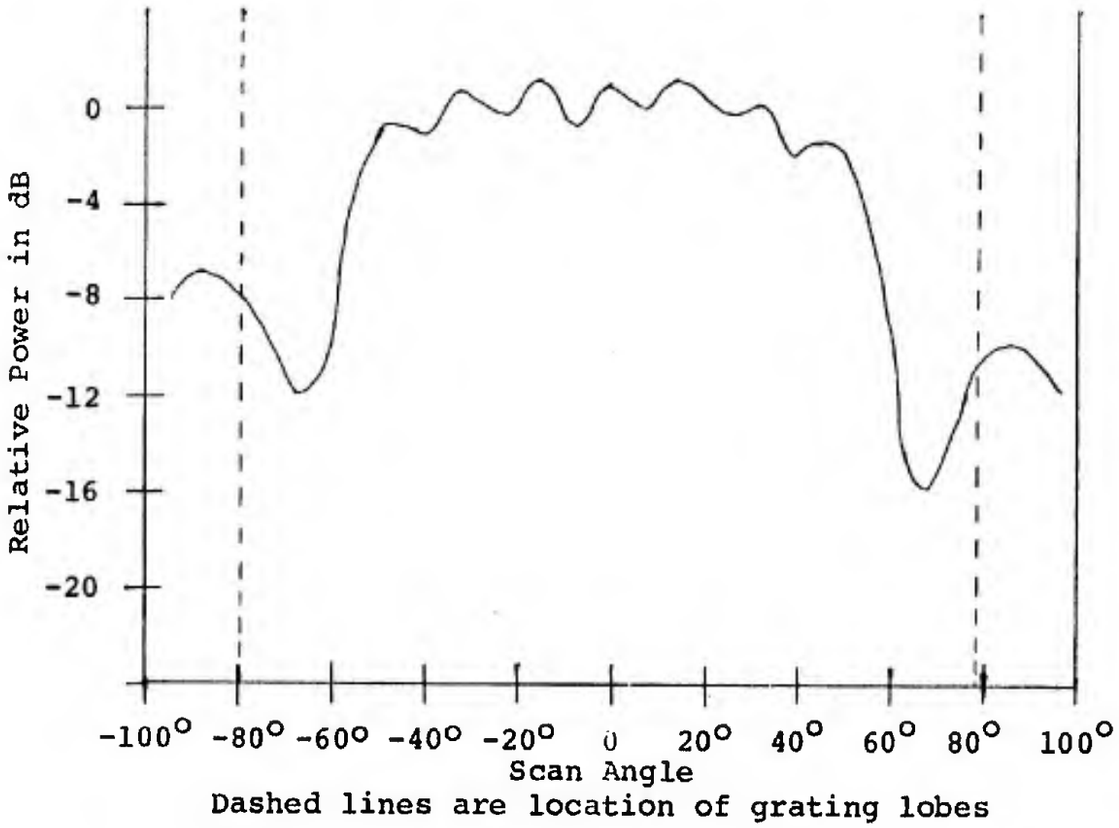

Fig. 16.--Element radiation pattern showing blind angles

obtained a measurement of this coupling through a mathematical process known as the induced emf method. He published his results in the form of an impedance that was dependent on the elements, their spacing and their geometry. In the intervening years others have made additions to Carter's results by considering more complicated geometries.[9]

In order to demonstrate the effect that this mutual impedance can cause, I considered the case of an array of two short dipoles* with the geometry shown in Figure 17. Then using the equivalent circuit of Figure 18 and results obtained from Jasik[10] the following equations for the load impedance Z_{Li} of each circuit were obtained.

$$Z_{L1} = Z_{11} + \frac{I_2}{I_1} Z_{12}$$

$$Z_{L2} = Z_{22} + \frac{I_1}{I_2} Z_{21} \qquad (26)$$

Where:

Z_{11}, Z_{22} = self impedance of the antenna element

Z_{12}, Z_{21} = mutual impedance between elements 1 and 2

I_1, I_2 = current flowing in the individual circuits

Since the antenna elements are identical

$$Z_{11} = Z_{22}$$

By reciprocity:

$$Z_{12} = Z_{21}$$

---

*This procedure is general and could be extended to n elements.

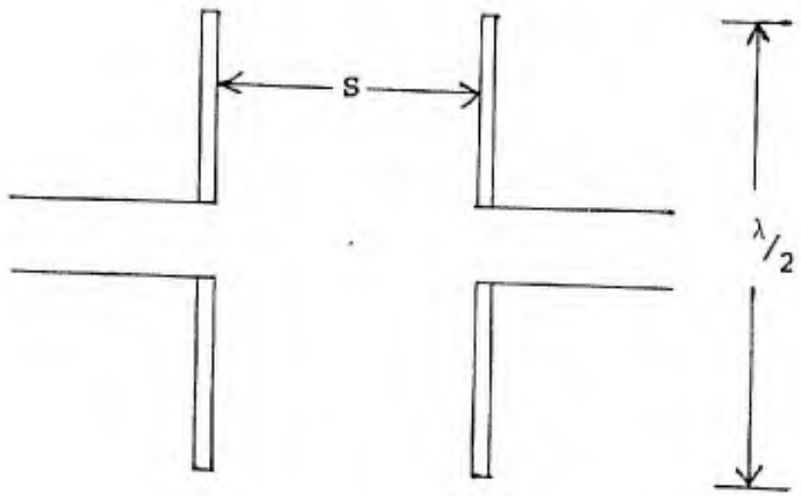

Fig. 17.--Geometry of dipoles for impedance calculation

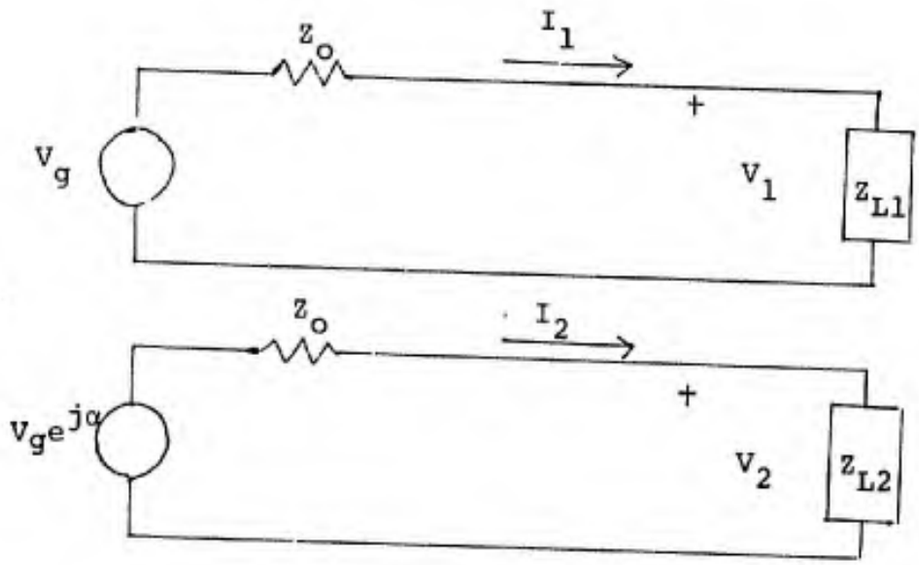

Fig. 18.--Equivalent circuit for load impedance

I used half wave dipoles with a self impedance of 72 ohms and assumed the circuits were matched to their generator with Z_o = 72 ohms. To phase the array I held one generator fixed and varied the phasing of the second. Figure 19 shows the impedance of one of the elements* as seen from the generator as a function of scan angle. Various curves are for different element spacings. I have also plotted the impedance that would be seen if there were no mutual coupling. It is apparent from this plot that the effect that mutual coupling has on the input impedance is considerable, and the fact that the majority of work on the blind angles considers mutual coupling to be the root cause of them is readily understood.

Of course, stating that mutual coupling is the root cause of blind angles is one thing; showing a physical relationship between them is an entirely different matter. However, what I have demonstrated so far should make it conceivable that a process does exist that changes the parameters of the system. And if we can change the parameters sufficiently, then we may be able to develop enough mis-match inside the system to cause a reflection coefficient approaching unity and consequently, a major reduction in the transmitted energy.

Surface Wave Theory

Though there have been many theories advanced as to the exact nature of the blind angle, there appear to be only two

---

*Only the result for one element is shown since the other element is identical and the results are the same, however, they are shifted in phase and reversed.

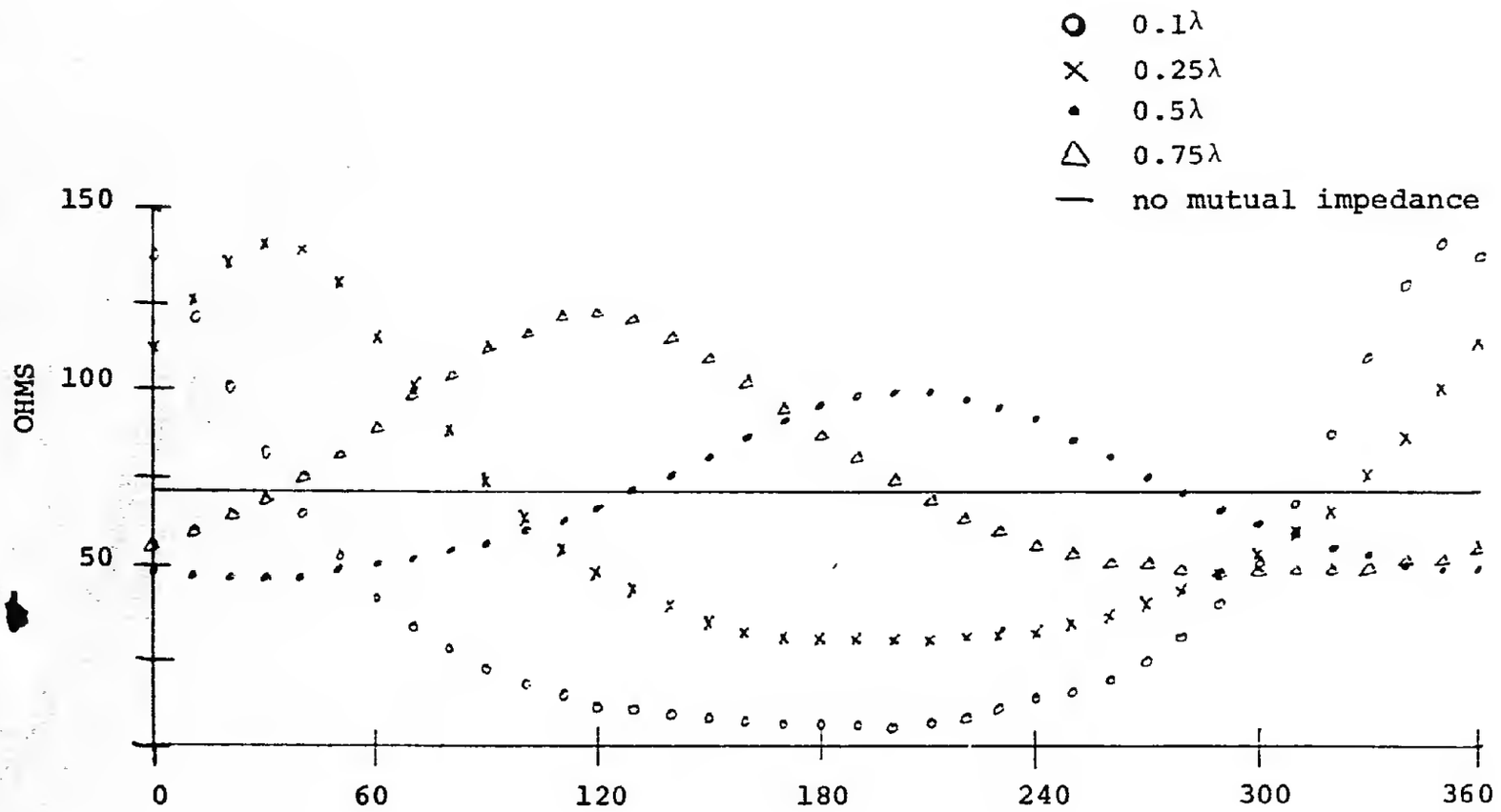

Fig. 19a.--Load resistance as a function of scan angle

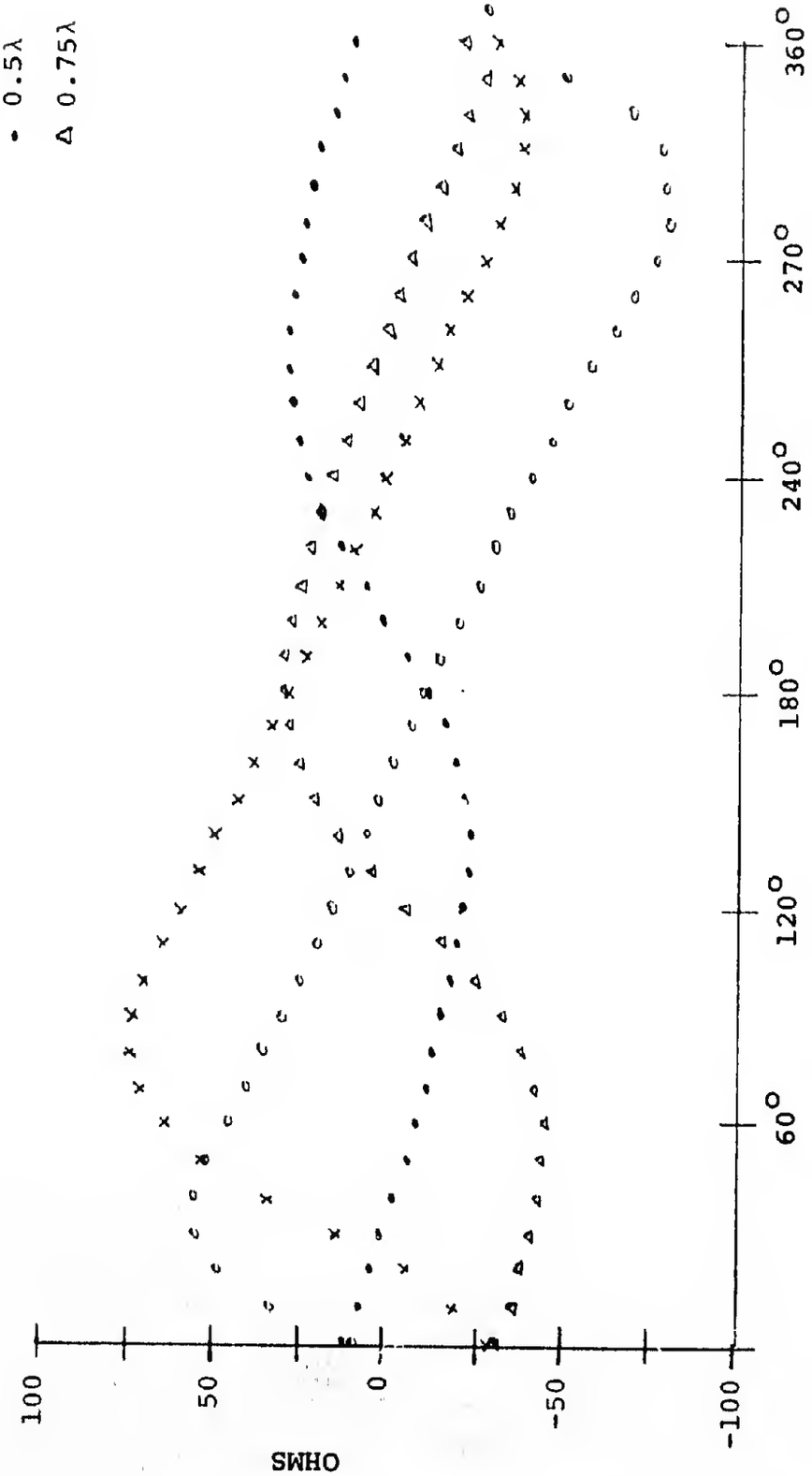

Fig. 19b.--Load reactance as a function of scan angle

major areas of inquiry that offer a physical explanation of it, --the surface wave and the modal theories. The surface wave concept is linked very closely with attempts to explain a means of mutual coupling and a reading of the available literature tends to indicate that this theory developed from attempts to explain that phenomenon. The concept and behavior of the surface wave is explained in considerable detail in many books and articles, see for example Waldron[11] and Barlow.[12] For our purposes, however, this type of wave is one which has an imaginary propagation constant along a surface, leading to propagation and a real propagation constant normal to the surface which demands attenuation from any component leaving the surface. These waves generally form at an interface between two dissimilar materials with different permitivity constants. They are especially apparent when a dielectric sheet is sandwiched between a perfect electric conductor and free space. The basic explanation using these waves is that the elements of the array cause a modification in the immediate surrounding medium. This modification takes the form of a changed refractive index which allows the existence of a surface wave. Bates[13] was one of the first to use the surface wave as an explanation. He assumed that the aforementioned condition existed to support the wave. These same conditions caused the apparent spacing of the elements to increase. This occurs because the velocity of the wave decreases in the modified region leading to a decrease in wavelength. This increased spacing can cause a grating lobe to move into the visible region

within the modified space. Since this grating lobe does not exist in free space, then the power in the grating lobe does not reach the free space region but is trapped along the array surface. Bates expected these grating lobes to coincide with the blind angles in the array. This idea became known as the "internal grating lobe."

Allen[14] also used the surface wave theory. However, he assumed that the elements of the array, in addition to being responsible for the modified environment, would both scatter and absorb energy from the surface wave. This interference would not be ϕ independent and hence would lead to preferred directions for the wave. Since this argument was applicable to each column in the array (assuming that the progressive phase shift exists for columns), there would be an accumulation of these effects. He called this effect coupling and assumed the accumulation would be significant along certain directions which corresponded to the blind angle.

A. Oliner[15] developed an important theory which I'll examine later but as a consequence he showed that the surface wave could only exist at those angles known as the blind angle. This, of course, has important ramifications for the entire surface wave theory. Both the surface wave and the blind angle occur simultaneously, negating a cause and effect relationship and implying the existence of some unknown causal factor.

Shortly after Oliner's work Lawrence Lechtreck, in an attempt to explain these angles, did some research on the

coupling between the elements. He theorized that the mutual coupling took place as a wave phenomena. To support this hypothesis he devised experiments in which he measured the coupling intensity and phase delay as a function of element spacing. His results support a uniform slow wave hypothesis for coupling. He suggests on the basis of his research a reason for the blind angle which is very similar to that proposed earlier by Allen. Briefly, he expresses a reflection coefficient for the array as a function of the coupling. He then demonstrates that the coupling adds out of phase and stays very small except at those particular angles where the blind angle exists. In those particular directions the coupling adds in phase and becomes significant--leading to a large reflection coefficient. An important point to Lechtreck's theory is that it appeared after Oliner and even while using some of his material, Lechtreck's research tends to indicate that the surface wave is always present in some degree, contrary to Oliner's hypothesis.

About a year later Oliner in collaboration with George Knittel and Alexander Hessel[16] published a paper in which they again examined the surface wave. Their conclusion was that the surface wave could only exist at the blind angle; the same conclusion Oliner had reached earlier. This time, however, they claimed that in reality the surface wave didn't exist. In its place they hypothesized the existence of a leaky wave. They claimed to show that this type of wave can exist at all times on the array surface and will cause the blind angle phenomena.

This latest theory not withstanding, Amitay et al., in 1972 published a book in which they reverted back to a type of surface wave to explain the coupling. They reported the leaky wave idea without comment and even went so far as to state that the surface wave as normally used can not be a lossless wave and hence, contradicts the surface wave assumptions. They used a form of a surface wave which they referred to as a forced surface wave but as I'll show later they displayed some ambivalence toward these results.

Modal Theory

The second major area, the modal theory, attempts to show the blind angle as a result of various propagating and attenuating modes. The existence of these various modes requires that different regions exist with different refractive indices. It is immediately evident that these are the same conditions required for the surface wave. In fact, as you will see, some of the researchers in this area have also done work in the surface wave area. Basically, this theory predicts that certain wave modes will exist in the dielectric but be below cut-off in air. Hence, if an equivalent network is developed for this array the modes that fail to exist in air will cause short circuits across the network leading to reflection coefficients of unit magnitude.

The basic work on this theory appears to have been done by A. Oliner and R. Malech. Their result is known as the "Ghost Mode Hypothesis," and I would like to present it in considerable detail since I believe it is a very important work. In this

report Oliner uses his unit cell technique. A unit cell can be thought of as a waveguide centered on the radiator and extending indefinitely in the direction of radiation. Its walls are E and H fields and are derived from the symmetry of the array and its excitation. These walls do not perturb the field distribution but are present because of field symmetries. Once the walls are present the field outside the unit cell may be completely ignored, allowing an examination of the array by looking at only one element. Oliner uses an array of narrow slots fed by rectangular waveguides and covered with a thin dielectric layer. A unit cell in this structure is depicted in Figure 20. The basis for his idea is that a number of propagating modes will exist in the dielectric material but will become evanescent once they enter the surrounding region of free space. He derives on the basis of this assumption an equivalent network to represent those that display this property. He uses an earlier derivation in which he shows that input contributions from individual modes can be represented by impedances that add directly in admittance form. In this particular hypothesis, Oliner designs a system in which only one propagating mode, the second order mode, meets the stated constraints. That is, the second order mode is the only mode that is present in the dielectric region and fails to exist in the free space region. This restriction allows him to represent the unit cell with the equivalent network of Figure 21. The two modes, first and second, are displayed as parallel transmission lines due to developing the equivalent network as an admittance. B in the network

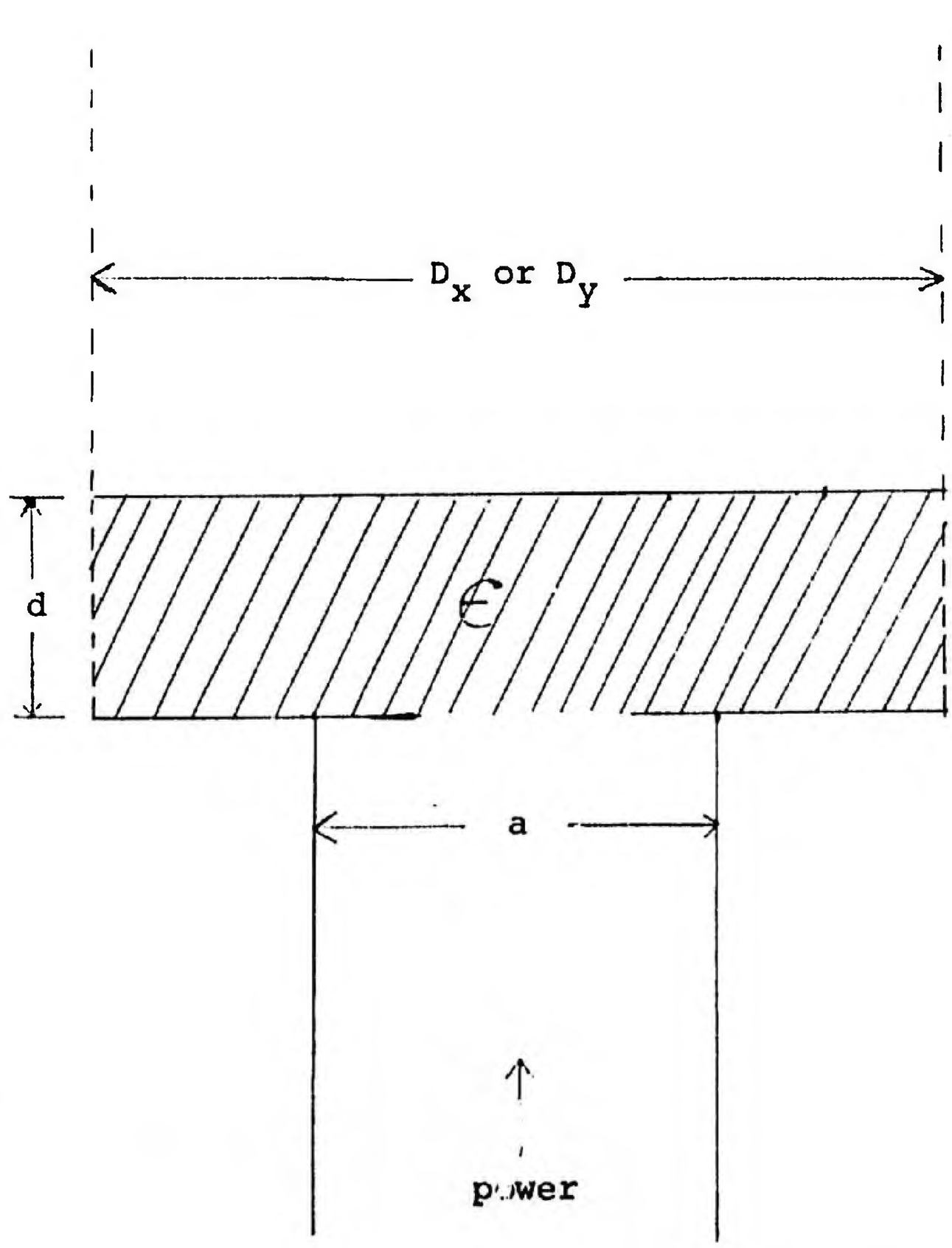

Fig. 20.--Unit cell of a slot array with a dielectric layer on the array face.

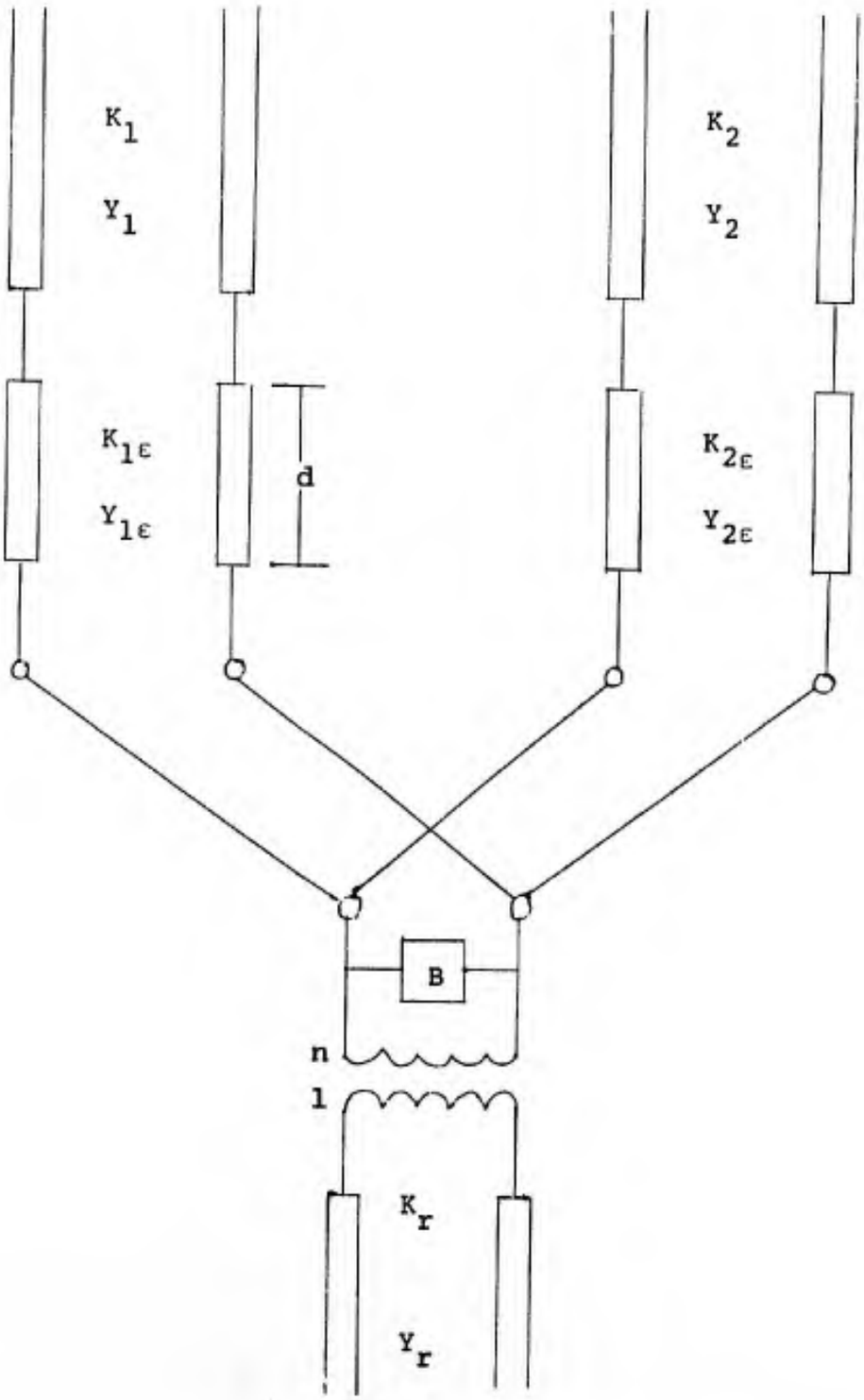

Fig. 21.--Equivalent network corresponding to the structure of Fig. 20, in which the two lowest modes are exhibited explicitly.

represents the susceptance of all higher order modes and the transformer is a means of depicting the feed system.

From simple transmission line relations, he develops the following equation for the normalized input admittance in the rectangular waveguide:

$$\frac{Y_a}{Y_r} = j\,\frac{B}{Y_r} + \frac{Y_{1\varepsilon}}{Y_r}\left[\frac{j+\left(\frac{Y_1}{Y_{1\varepsilon}}\right)\cot K_{1\varepsilon}d}{\cot K_{1\varepsilon}d + j\left(\frac{Y_1}{Y_{1\varepsilon}}\right)}\right]\left|\frac{V_{1\varepsilon}}{V_r}\right|^2 + \frac{Y_{2\varepsilon}}{Y_r}\left[\frac{j+\left(\frac{Y_2}{Y_{2\varepsilon}}\right)\cot K_{2\varepsilon}d}{\cot K_{2\varepsilon}d + j\left(\frac{Y_2}{Y_{2\varepsilon}}\right)}\right]\left|\frac{V_{2\varepsilon}}{V_r}\right|^2 \tag{27}$$

$\left|\frac{V_{1\varepsilon}}{V_r}\right|^2$ and $\left|\frac{V_{2\varepsilon}}{V_r}\right|^2$ are related to the transformer and can be ignored because they are well behaved. The term containing Y_1 and $Y_{1\varepsilon}$ corresponds to the first mode and also can be ignored since it exhibits no rapidly varying behavior.

However, looking at the second mode some interesting occurrences take place. Since by assumption propagation occurs in the dielectric, $Y_{2\varepsilon}$ and $K_{2\varepsilon}$ are real; Y_2 is imaginary, however, because the mode does not propagate in the free space region. Therefore the factor

$$\frac{j + \frac{Y_2}{Y_{2\varepsilon}}\cot K_{2\varepsilon}d}{\cot K_{2\varepsilon}d + j\left(\frac{Y_2}{Y_{2\varepsilon}}\right)}$$

is purely imaginary. It offers no contribution to the active conductance. In fact, it must propagate in free space and

carry away real power before it makes any contribution to the conductance.

The susceptance, however, is affected. Oliner shows that the form of Y_2 and $Y_{2\varepsilon}$ are dependent on the plane (E or H) of scan. He shows that they can be represented by:

$$Y_{2\varepsilon} = \frac{\omega \varepsilon_o \varepsilon'}{K_{2\varepsilon}} \tag{28}$$

$$Y_2 = \frac{\omega \varepsilon_o}{K_2} = j \frac{\omega \varepsilon_o}{|K_2|} \tag{29}$$

for E plane and

$$Y_{2\varepsilon} = \frac{K_{2\varepsilon}}{\omega \mu} \tag{30}$$

$$Y_2 = \frac{K_2}{\omega \mu} = -j \frac{|K_2|}{\omega \mu} \tag{31}$$

for H plane, where ε' is the relative dielectric constant of the layer. For the E plane scan the factor becomes:

$$j \left[\frac{1 + \left(\frac{K_{2\varepsilon}}{\varepsilon' |K_2|} \right) \cot K_{2\varepsilon} d}{\cot K_{2\varepsilon} d - \left(\frac{K_{2\varepsilon}}{\varepsilon' |K_2|} \right)} \right] \tag{32}$$

You can see that it is possible for the denominator to go to zero when

$$\cot k_{2\varepsilon} d = \frac{K_{2\varepsilon}}{\varepsilon' |K_2|} \tag{33}$$

When this occurs the numerator is finite, hence, the susceptance becomes infinite and the array plane becomes a short circuit.

Since the active reflection coefficient is related to the active admittance by:

$$\Gamma_a = \frac{1 - \frac{Y_a}{Y_r}}{1 + \frac{Y_a}{Y_r}} \tag{34}$$

the reflection coefficient $|\Gamma_a|^2 = 1$. Hence we have a total reflection of the wave, and an element null at the angle for which (33) is satisfied. By using the relationships

$$k_{xo} = k \sin \theta \tag{35}$$

$$K_{mn} = \left[k^2 - \left[k \sin \theta + \left(\frac{2\pi}{D_x}\right) m\right]^2\right]^{\frac{1}{2}} \tag{36}$$

and writing the wave numbers in terms of the angle θ he obtains this null angle as:

$$\frac{K_{2\epsilon}}{k} = \left[\epsilon' - \left[\sin \theta - \left(\frac{\lambda}{D_x}\right)\right]^2\right]^{\frac{1}{2}} \tag{37}$$

$$\left|\frac{K_2}{k}\right| = \left[\left[\sin \theta - \left(\frac{\lambda}{D_x}\right)\right]^2 - 1\right]^{\frac{1}{2}} \tag{38}$$

His claim then is that this angle must be nearer to broadside than the angle corresponding to the onset of the grating lobe because K_2 is still imaginary for it.

He goes on to show the same occurrences for the H plane with the added requirement that d, the thickness of the dielectric, must be larger than for the E plane scan. What he has demonstrated is the existance of a null in the array pattern prior to the onset of the grating lobe--a blind angle!

And not only has he demonstrated its existence but he has provided a means of prediction. I believe this particular work is of considerable importance because it, for the first time, offers some reasonable explanation as to what precisely is occurring.

In Knittel's paper in which he proposed the leaky wave concept, he also examined the blind angle using this ghost-mode. He agreed that this was the proper format for explaining the phenomenon but he concluded that the original idea needed refinements. He confined these modifications to studying higher order modes and changes in the susceptance they caused. He also more fully examined the entire range of the phasing and its effect on the equivalent circuit. The importance of this paper, however, is that it does support the original theory and extends it without any major modifications. This, of course, does not imply that the problem has been adequately explained. Quite the contrary, serious problems still continued to exist. The way the equivalent network was developed tends to indicate that the blind angle is directly proportional to the inter-element spacing, i.e., the closer the spacing the closer to broadside is the angle. This appears logical since the mutual impedance data published by Carter and others showed that the impedance, although oscillatory, increased in amplitude with the highest value located at the closest spacing. In practice, however, the blind angle reaches a minimum separation from broadside and closer element spacing moves it out.[14] Wasylkiwskyj[17] confirmed that the overall coupling (not impedance) in the array peaked at some inter-element spacing and then decreased with a further

decrease in spacing. Unfortunately, this fact did not seem apparent or even implied in the two theories.

An examination of these theories shows that they are both related to solving the boundary value problem at the interface of the array and the surrounding medium--i.e., matching the modes on both sides. The two authors have both assumed the existence of a single mode in the feed line. Amitay, et al., demonstrated that this use of a single mode was undependable. He showed that the problem could be more accurately made to conform with empirical data by incorporating more modes. For his publication he studied up to eighteen modes for the feed and instead of producing an equivalent network he solved the boundary value problem with integral equations.

Later, Louis Stark[18] published a paper in which he reported that he could predict the location of the blind angle and also show that it did not continue to move toward broadside monotonically as the spacing decreased. The developed equation is shown here and the physical geometry of the array is shown in Figure 22.

$$\frac{1-\Gamma}{1+\Gamma} = \frac{1}{\eta}\left\{Y_{11} + \frac{Y_{12}Y_{21}}{jY-Y_{22}}\right\} \tag{39}$$

where

$$Y_{11} = \eta_o \frac{\delta L}{2ab} \sum_{m=-\infty}^{\infty} \sum_{n=-\infty}^{\infty} \frac{k^2-h_n^2}{k\gamma_{m,n}} I_1^{mn} I_1^{*mn}$$

$$Y_{12} = \eta_o \frac{\delta L}{2ab} \sum_{m=-\infty}^{\infty} \sum_{n=-\infty}^{\infty} \frac{k^2-h_n^2}{k\gamma_{m,n}} I_1^{mn} I_2^{*mn}$$

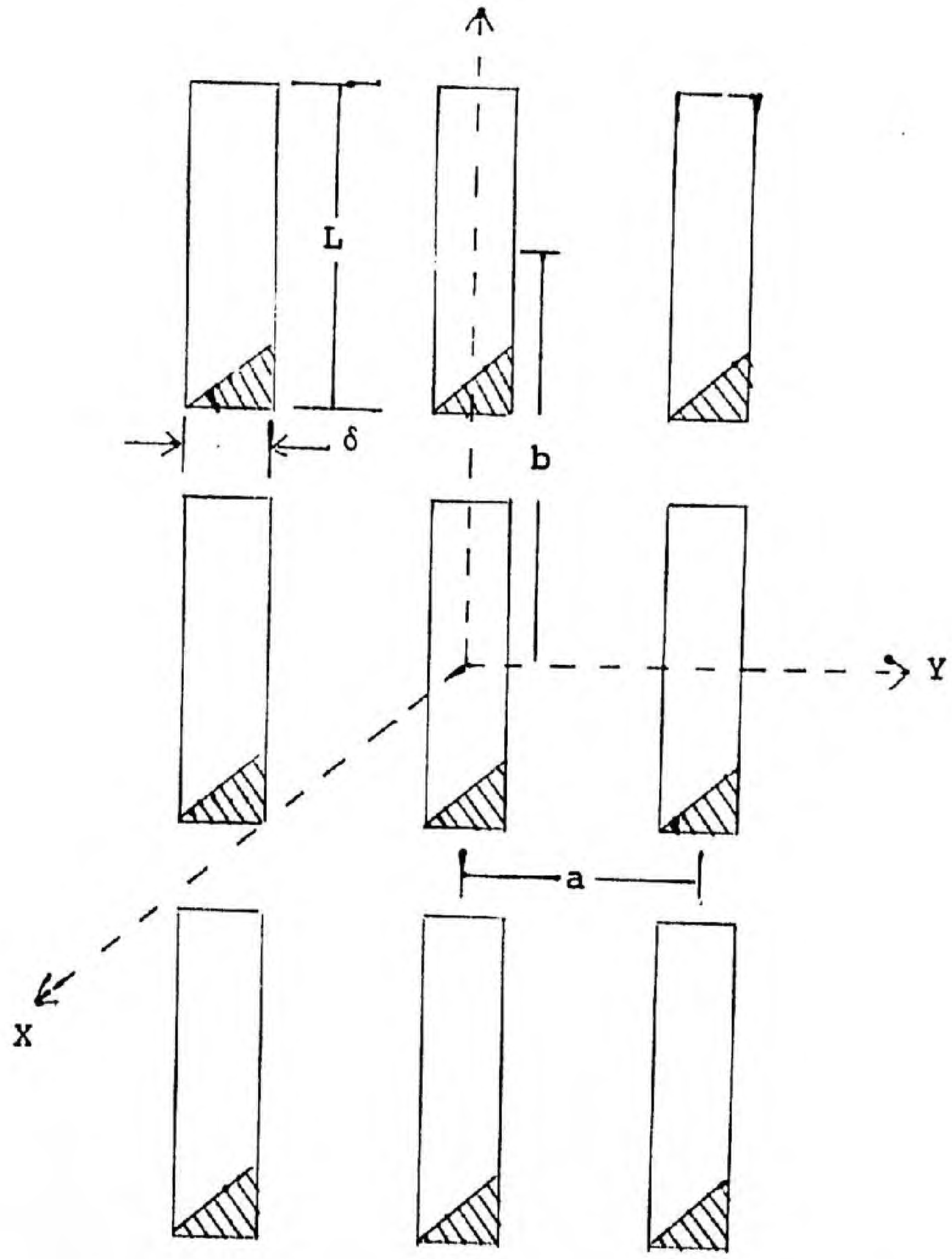

Fig. 22.--Geometry of array used to develop Stark's equations.

$$Y_{21} = \eta_o \frac{\delta L}{2ab} \sum_{m=-\infty}^{\infty} \sum_{n=-\infty}^{\infty} \frac{k^2 - h_n^2}{k\gamma_{m,n}} {}^{*}I_1^{mn} I_2^{mn} = -Y_{12}$$

and

$$Y_{22} = \eta_o \frac{\delta L}{2ab} \sum_{m=-\infty}^{\infty} \sum_{n=-\infty}^{\infty} \frac{k^2 - h_n^2}{k\gamma_{m,n}} I_2^{mn} {}^{*}I_2^{mn}$$

where:

$\frac{1 - \Gamma}{1 + \Gamma}$ = normalized driving point admittance

$$I_i^{mn} = \frac{2}{\delta L} \iint_{slot} \exp(-jB_m y)\, dy \cos \frac{\pi z}{L} \exp(-jh_n z)\, dz$$

jY = wave susceptance of next higher mode

η = wave admittance of the $TE_{1,0}$ mode

δ = width of element in y direction

L = length of element in x direction

a = spacing between centers of elements in y direction

b = spacing between centers of elements in x direction

k = free space wave number

h = propagation constant in z direction

γ = propagation constant in x direction

The particular angle at which the equation goes to infinity is found from the relations:

$B_m = k \left[\cos \theta_y{}^{oo} + \frac{m\lambda}{a}\right]$; $\cos \theta^{oo}$ = direction cosine of principle wave

$h_n = k \left[\cos \theta_z{}^{o,o} + \frac{n\lambda}{b}\right]$

An important point to note is that the (Y_{11}) term was derived by using only a single mode--like Oliner and Knittel. The second term is a correction factor introduced by the next higher mode thereby showing the coupling relationship that Wasylkiwskyj reported.

Other Work

Most other research during the last ten years has taken the attitude that the blind angle exists, that it is caused by some form of mutual coupling, and that the problem, therefore, is to avoid it or limit its effects. Although many papers using this approach have been published, there are two that I believe illustrate the theories I have presented. The first written by Agrawal[19] is primarily based on Allen's and Lechtreck's theories of a summation of coupling terms. Agrawal accepts the theory that the summation is caused by the periodicity of the array. He attacks the problem by destroying this periodicity. Using a probability technique he designs an array with random spacing between the elements. His procedure works and he succeeds in eliminating the blind angle lending credence to the surface wave concept.

S. W. Lee,[20] on the other hand, approaches the problem by looking at the modal theory. Through the incorporation of an inductive iris within the open end of the feed waveguide, he succeeds in changing the mode structure of the radiating elements. This change in structure forces the blind angle to move further from broadside than the one radiated by the unmodified structure.

Through the use of integral equations and mode matching he is able to predict this change.

CONCLUSION

I believe that it is safe to state that the blind angle is definitely caused by mutual coupling. The coupling can be represented by many different ways be it mutual impedance, coupling coefficients or scattering parameters. Regardless of which we wish to use, we must eventually develop a reflection coefficient of unity to support the blind angle. The ghost mode hypothesis and its subsequent theory (Knittel, Stark) offer a physical insight into the problem which appears at this stage to be, if not the correct explanation, at least one that answers most questions and offers a good chance of accurate predictions. As far as the coupling itself is concerned, the various authors have shown that it is affected by element size, spacing, dielectric constant of the surrounding medium, and the periodicity of the array structure. Whether it is actually a surface wave or a leaky wave or something entirely different is not definitely known. Our understanding in research today is probably best demonstrated by two statements:

1) Amitay, et al., states in 1972, "Our understanding of the array resonance phenomenon is still incomplete."
2) M. T. Ma,[21] published a book in 1974 on phased array radars in which he totally ignores blind angles.

APPENDIX I

Refer to Figure 23. Assume we know α, R and d. We need to find B and γ and compare them.

$$\gamma = \arctan \frac{B}{A}$$

$$B = [R \times \sin \alpha] - d$$

$$A = R \times \cos \alpha$$

$$\gamma = \arctan \frac{[R \times \sin \alpha] - d}{R \times \cos \alpha}$$

$$B = \arctan \frac{B + 2d}{A}$$

$$= \arctan \frac{[R \times \sin \alpha] - d + 2d}{R \times \cos \alpha}$$

$$B = \arctan \frac{[R \times \sin\alpha] + d}{R \times \cos \alpha}$$

Making use of an inverse trig function relationship,[22] I can show the difference between the angles γ,B; γ,α; α,B

$$\gamma - B = \arctan \frac{B}{A} - \arctan \frac{B+2d}{A}$$

$$= \arctan \frac{\frac{B}{A} - \frac{B + 2d}{A}}{1 + \frac{B}{A} \cdot \frac{B+2d}{A}}$$

$$= \arctan \frac{\frac{2d}{A}}{\frac{A^2+B^2+2Bd}{A^2}} = \arctan \frac{2Ad}{A^2+B^2+2Bd}$$

$$= \frac{2dR \cos \alpha}{R^2 \cos^2 \alpha + R^2 \sin^2\alpha + d^2 - 2Rd \sin \alpha + 2Rd \sin \alpha - d^2}$$

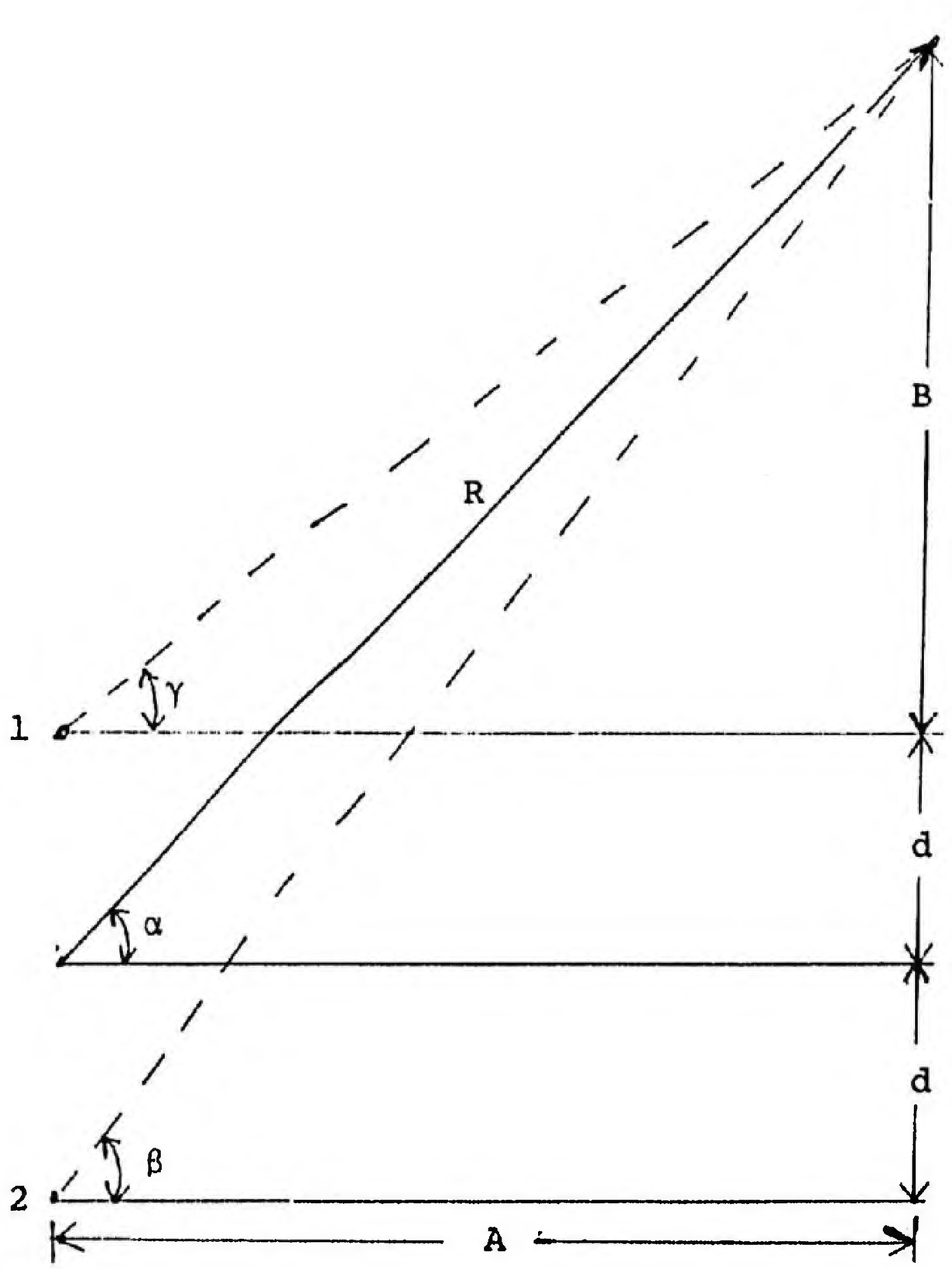

Fig. 23.--Individual Signal Paths

$$= \arctan \frac{2dR \cos \alpha}{R^2(\cos^2\alpha + \sin^2\alpha)}$$

$$\gamma - B = \arctan \frac{2d \cos \alpha}{R}$$

If we examine the worst possible case, i.e., $\alpha = 0^o$ or 180^o then the difference is:

$$\arctan \frac{2d}{R}$$

If $d = \lambda/2$ and $R = 10\lambda$ then the difference is:

$$\arctan \frac{1}{10} = 5.7^o$$

If $d = \lambda/2$ and $R = 100\lambda$ then the difference is:

$$\arctan \frac{1}{100} = .57^o$$

For a frequency of 100 M H Z a distance of 100λ is only 300 meters. The difference between λ and α using the same procedure as above yields:

$$\frac{d \cos \alpha}{R - d \sin \alpha}$$

Again looking at the worst possible case ($\alpha = 0$) this yields:

$$\arctan \frac{d}{R} = \frac{1}{2} (\gamma - B)$$

Therefore, if R is much greater in terms of wavelengths than d, the approximation of parallel lines is quite accurate.

APPENDIX II

To obtain the equality:

$$\left|\frac{1 - e^{-jn\psi}}{1 - e^{-j\psi}}\right| = \left|\frac{\sin \frac{n\psi}{2}}{\sin \frac{\psi}{2}}\right|$$

Proceed as follows:

1) $$\left|\frac{1 - e^{-jn\psi}}{1 - e^{-j\psi}}\right| = \left|\frac{1 - e^{-2j\frac{n\psi}{2}}}{1 - e^{-2j\frac{\psi}{2}}}\right| = \left|\frac{e^{j\frac{\psi}{2}}}{e^{j\frac{n\psi}{2}}}\right| \left|\frac{e^{j\frac{n\psi}{2}} - e^{-j\frac{n\psi}{2}}}{e^{j\frac{\psi}{2}} - e^{-j\frac{\psi}{2}}}\right|$$

2) $$\left|\frac{e^{j\frac{\psi}{2}}}{e^{j\frac{n\psi}{2}}}\right| = \left|e^{j\frac{\psi}{2}(1-n)}\right| = 1$$

3) $$\left|\frac{e^{j\frac{n\psi}{2}} - e^{-j\frac{n\psi}{2}}}{e^{j\frac{\psi}{2}} - e^{-j\frac{\psi}{2}}}\right| = \left|\frac{\sin \frac{n\psi}{2}}{\sin \frac{\psi}{2}}\right|$$

$$\therefore \left|\frac{e^{j\frac{\psi}{2}}}{e^{j\frac{n\psi}{2}}}\right| \left|\frac{e^{j\frac{n\psi}{2}} - e^{-j\frac{n\psi}{2}}}{e^{j\frac{\psi}{2}} - e^{-j\frac{\psi}{2}}}\right| = (1) \left|\frac{\sin \frac{n\psi}{2}}{\sin \frac{\psi}{2}}\right|$$

and the proof is complete.

REFERENCES

1. N. Rao, "Basic Electromagnetics with Application." Englewood Cliffs, New Jersey: Prentice-Hall Inc., 1972, pp. 489-500.

2. W. Hayt, Jr., "Engineering Electromagnetics." New York: McGraw Hill, 1974, pp. 454-463.

3. E. Jordan and K. Balmain, "Electromagnetic Waves and Radiating Systems." Englewood Cliffs, New Jersey: Prentice-Hall Inc., 1968, pp. 362-363.

4. Kaplan, "Advanced Calculus." Reading, Mass: Addison-Wesley Publishing Co., Inc., 1952, p. 316.

5. W. Weeks, "Antenna Engineering." New York: McGraw-Hill, 1968, p. 73.

6. L. Lechtreck, "Effects of Coupling Accumulation in Antenna Arrays." IEEE Trans. Antennas Propagation, Vol. AP-16, pp. 31-37, Jan. 1968.

7. N. Amitay, V. Galindo, and C. P. Wu, "Theory and Analysis of Phased Array Antennas." New York: Wiley-Interscience, 1972, pp. 14-15, pp. 200-213, pp. 237-259, pp. 200-207, p. 259.

8. P. Carter, "Circuit Relations in Radiating Systems and Application to Antenna Problems." Proc. IRE, Vol. 20, pp. 1004-1041, Jan. 1932.

9. H. Baker and A. LaGrone, "Digital Computation of the Mutual Impedance Between Thin Dipoles." IEEE Tran. Antennas Propagation, Vol. AP-10, pp. 172-178, March 1962.

10. H. Jasik, "Fundamentals of Antennas." In "Antenna Engineering Handbook." H. Jasik, ed., New York: McGraw Hill, 1961, pp. 2-11-2-13.

11. R. Waldron, "Theory of Guided Electromagnetic Waves." London: Van Nostrand Reinhold Co., 1969, pp. 359-375.

12. H. Barlow and A. Cullen, "Surface Waves." Proc. IEE (London), Vol. 100, pt. 3, pp. 329-347, Nov 1953.

13. R. Bates, "Mode Theory Approach to Arrays." IEEE Trans. Antennas Propagation, Vol. AP-13, pp. 321-322, March 1965.

14. J. Allen, "On Surface Wave Coupling Between Elements of Large Arrays." IEEE Trans. Antennas Propagation, Vol. AP-13, pp. 638-639, July 1965.

15. A. Oliner and R. Malech, "Mutual Coupling in Infinite Scanning Arrays." In "Microwave Scanning Antennas." R. Hansen, ed., New York: Academic Press, Inc., 1966, Vol.II, Chapter 3.

16. G. Knittel, A. Hessel and A. Oliner, "Element Pattern Nulls in Phased Arrays and Their Relation to Guided Waves." IEEE Proceedings, Vol. 56, No. 11, pp. 1822-1836, Nov 1968.

17. W. Wasylkiwskyj and W. Kahn, "Mutual Coupling and Element Efficiency for Infinite Linear Arrays." IEEE Proceedings, Vol. 56, No. 11, pp. 1901-1907, Nov. 1968.

18. L. Stark, "Microwave Theory of Phased Array Antennas--A Review." IEEE Proceedings, Vol. 62, No. 12, pp. 1661-1701, Dec 1974.

19. V. Agrawal, "Mutual Coupling in Phased Arrays in Randomly Spaced Antennas." Ph.D. Dissertation, Dept. of Electrical Engineering, University of Illinois, Champaign, Illinois 1971.

20. S. W. Lee and W. Jones, "On the Suppression of Radiation Nulls and Broadband Impedance Matching of Rectangular Waveguide Phased Arrays." IEEE Trans. Antennas Propagation, Vol. AP-19, No. 1, pp. 41-51, Jan 1971.

21. M. T. Ma, "Theory and Application of Antenna Arrays." New York: Wiley-Interscience, 1974.

22. R. Hudson, "The Engineers Manual." New York: John Wiley and Sons, Inc., 1944, p. 12.